We thank the referees for their comments on the manuscript and for the many useful suggestions that helped us in preparing an improved version of the manuscript.

In the following, we address their comments.

Referee #1

Main comments

1. The 20th Century ensemble reanalysis at 2.0 degrees is used as boundary conditions for simulations with a 25km (~0.22 degree) outer domain. In the analysis, the poor alignment of the convergence zones is attributed to the low resolution of the reanalysis but this could be mitigated by introducing a WRF domain with 125km. This should be attempted at least for the four members analysed

Reply: It is true that the ratio of the grid spacing for the driving data to that of our outer 25 km domain (roughly 1:9) is larger than what is normally recommended, and larger than the 1:5 ratio we use for our inner domains. Because of the large computational cost to run 56 ensemble members with each one including a refined 1 km domain, the decision originally had been made to only use 3 nests. Because we no longer have access to such a large amount of computer resources, we are unable to re-run all 56 members, but we recognize that the reviewer raises an interesting question. Therefore, with the limited resources remaining, we have chosen to re-run the 4 best members (1, 13, 22 and 37) adding a fourth outer domain with 125 km grid spacing (in addition to 25, 5, and 1 km grid spacing) (see Fig. 1).

The comparison of 36 hour QPF for the innermost domain at 1 km grid spacing is provided in Figure 2: first row results corresponding to simulations driven by outermost domain at 25 km grid spacing, second row the same but with outermost domain at 125 km grid spacing. Heavier areal QPF can be seen in all members in the first row (our original configuration), both on the entire 1 km grid spacing domain (both on sea and land areas), and also on the smaller area over which the paper focuses.

This statement is confirmed when comparing, for the 4 selected best members, the BIAS and MAE (in mm) over the available 64 raingauge stations in the runs using an outermost domain with 25 and 125 km grid spacing respectively (Table 1).

Member	BIAS-d01 25 km	BIAS-d01 125 km	MAE-d01 25 km	MAE-d01 125 km
1	-19.8	-30.0	38.4	38.9
13	-14.6	-26.4	40.5	42.2
22	-21.8	-29.8	39.9	45.9
37	-18.2	-26.9	42.1	44.6

Table 1. - BIAS and MAE (in mm) for the 4 selected best member ensembles over the available 64 raingauge stations in the runs having an outermost domain with 25 and 125 km grid spacing, respectively.

The New Simplified Arakawa-Schubert (NSAS) scheme adopted in these additional simulations over the 125 and 25 km grid spacing domains has been revised, for deep moist convection, to make cumulus convection stronger and deeper to deplete more instability from the atmospheric column and result in the suppression of excessive grid-scale precipitation (Han and Pan, 2011). This can result, if applied even at very coarse grid spacing (125 km), in an overall reduction of the efficiency of the precipitation processes, thus impacting also the results on the innermost domains down to 1 km grid spacing.

We therefore believe it is advantageous to maintain our previously obtained results and to not introduce the extra 125 km domain, which adversely affects results, likely because of the NSAS scheme that we use.

2. The advantage of high resolution simulations is their ability to provide 3D information of an event. No analysis of the upper air results, vertical profiles or 2D vertical cross-sections has been presented. The dynamics of the storm evolution should be added to the manuscript.

Reply: the physical mechanism responsible for the generation of the back-building MCS observed on 25 september 1915 also has been recently explained by Fiori et al. (2017). Taking advantage of the availability of both observational data and modelling results at the micro-α meteorological scale, Fiori et al. (2017) provide insights about the triggering mechanism and the subsequent spatio-temporal evolution of the Genoa 2014 back-building MCS. The major finding is the important effect of a virtual mountain created on the Ligurian sea by the convergence of a cold and dry jet outflowing from the Po valley and a warm and moist low level south-easterly jet within the PBL.

The same mechanism is active also for this case. Let us consider, as an example, the convective flow field at 06UTC on 25 september 1915 (see Figure 3), as predicted by member 1 of the ensemble. Panel A shows the 2 m potential temperature field together with the 10 m horizontal wind vector field: the colder and drier jet outflowing from the Po valley and the warmer and moister air from southern mediterranean sea are evident. Panel B shows, by means of the potential temperature along the cross section corresponding to the green dotted line of Panel A, also the thin potential temperature layer (virtual mountain) in front of the actual Liguria topography. This acts, in agreement with Fiori et al. (2017), to produce the strong convective cells in panel C (updraft velocity above 10 m/s) with the apparent back-building on the western side (less mature and intense cells around 8.4° latitude). The main updraft produces vertical advection of water vapor (panel D), thus resulting in significant production of rainwater (panel E), snow (panel F, significantly advected inland by the upper level south-westerly winds), and graupel (panel G).

This analysis in now included in the revised version of the manuscript.

3. Although an ensemble of 56 members is produced, only 2 deterministic measures of individual ensemble members are presented but no analysis of the quality of such ensemble is provided. A shortcoming of deterministic measures of skill is that information about prediction uncertainties is not available, thus categorical measures like Brier skill score, continuous ranked probability score, ROC skill score are a useful tool to assess the quality of an ensemble forecast. In the following references examples such types of analysis can be found. Please add some categorical measures.

Reply: It is well know (Mass et al. 2002) that point-to- point verification measures like those usually used for traditional ensemble verification do not work well with fine grid spacing simulations, because a double penalty exists for spatial errors, which are extremely common for high intensity precipitation events. This problem is likely even worse when limited observations from 1915 are used. Object-based verification techniques have been developed in the last 10-15 years specifically because of these problems. The application of the MODE Object-based verification technique showed that twelve members out of the 17 members selected using the minimum divergence criterion have significant values (above 0.8) of the total interest function. Specifically, when examining paired observed and modelled clusters, these twelve members demonstrate useful skill for: centroid distance, providing a quantitative sense of spatial displacement of forecast; forecast area/observed area, providing an objective measure of over-or under-prediction of areal extent of the forecasts; forecast intensity 50/observed intensity 50 and forecast intensity 90/observed intensity 90, providing objective measures of median (50th percentile) and near-peak (90th percentile) intensities found in the objects; and the already mentioned total interest, a summary statistic derived from the fuzzy logic engine with user-defined interest maps for all these attributes plus some others (Tab. 2).

Parameter	Average	Standard deviation
PAIRED CENTROID DISTANCE (km)	114	62
FCST AREA/OBS AREA	1.10	0.90
FCST INT 50/OBS INT 50	0.73	0.06
FCST INT 90/OBS INT 90	0.62	0.11
TOTAL INTEREST	0.88	0.09

Where:
CENTROID DISTANCE: provides a quantitative sense of spatial displacement of forecast.
FCST AREA/OBS AREA: provides an objective measure of whether there is an over-or under-prediction of areal extent of forecast.
FCST INT 50/OBS INT 50 and FCST INT 90/OBS INT 90 provide objective measures of Median (50th percentile) and near-Peak (90th percentile) intensities found in objects.
TOTAL INTEREST: provides summary statistic derived from fuzzy logic engine with user-defined interest maps for all these attributes plus some others.

Table 2. - Clusters pairs statistics for the 12 members out of 17, showing significant values (above 0.8) of the total interest function.

This results are now included and discussed in the revised version of the manuscript.

4. The deterministic measures are also evaluated by comparing observations and simulations with different time spans. In lines 209-218 reference is made to rainfall depths for a 4 hour period thus QPE should be computed for the same time period as the simulation and only then should the evaluation be performed. In case that is not possible, the simulation should cover the same time period of the observations.

Reply: A comparison at an hourly level is basically meaningless (due to high variability within the simulations) and also impossible (no observational data are available on

hourly scales). Furthermore the 12 hours covered by the observations and not covered by the model do not experience important precipitation (as supported with the notes on the past weather in the daily bulletins (e.g. "pioggia dal mattino" or "pioggia fino al pomeriggio"). Additionally the QPF in all 56 members for the period 12 UTC 24th – 00 UTC 25th is negligible over the entire Liguria Region (averaging below 1 mm in 12 hours). Therefore, verification statistics using the time periods we have chosen would not differ meaningfully from those performed if we had access to observations whose timing did match exactly the simulation period. We will mention this in the revised version of the manuscript.

Minor comments

Figures 3 is very difficult to read. Since its quality cannot be enhanced I would suggest adding a figure 3b with the ensemble mean slp with the same domain and isobar resolution in order to better assess the resemblance between the 20th Century Reanalysis and the forecasted conditions on the 25th of September. The approximate pressure gradients in the Po Valley, Mediterranean and France, in both analysis, would be appreciated.

Reply: Done.

Figure 4c is as difficult to read as figure 3. Figures 4a and b should represent the same domain as figure 4c. Same argument as before**.**

Reply: Done.

In lines 209-218 reference is made to rainfall depths for a 4 hour period. If sub-daily precipitation is available please add either QPE or individual stations time series for the periods analysed in figures 10 and 11.

Reply: Sub-daily precipitation is not available.

The topography of the WRF plays a fundamental role in the development of the convective system but is missing from the manuscript. I suggest replacing the map in figure 8 with the model topography for all the domains.

Reply: Done.

To facilitate the comparison with the real topography, I would suggest the merger with figure 1 as figure 1b. Also in figure 1 there is no reference to the source of the topographic map.

Reply: the prefer keeping figure 1 as it is, in order to avoid introducing in the introduction section a reference to technical issue that is presented only in section 3.

Lines 95-100 – Paragraph is too long, please rephrase.

Reply: Done.

Line 170 – The paragraph refers to 500hPa chart, i.e. figure 2b Line 178 – Should be figure 2a, not 2b Line 746

Reply: we corrected the mistake.

Y axis in figure 9 difficult to read. Reduce the resolution and increase the caption font.

Reply: We have added the measurement unit to the figure caption.

Line 755 – Indexation of figure 10 and 11, hard to follow. Attribute the indices sequentially. Legend should describe better the individual panel figures.

We improved the captions of figures 10 and 11. It was however not possible to attribute the indices sequentially because the 6 panels in figure 10 and the 6 ones in figure 11 refer to different ensemble members.

Referee #2

Main comments

1. Even if 56 members on the 20th century reanalysis were studied, only four of them reproducing the best the event's dynamics were taken into account while showing the results. It would be interesting to have some comments about the members showing very "non-realistic dynamics" and also about the mean ensemble.

Reply: some information on the other members would indeed be interesting, but we prefer keeping the focus of the paper which investigates the ability of the ARF-WRF simulations to capture the MCS character of the event. The members showing very "non-realistic dynamics" and also the mean ensemble fail to capture the convergence line creation and its evolution responsible for the generation of the back-building MCS in 17 out of 56 members. We prefer therefore not discussing them in order to keep the focus of the paper on the back-building MCS character of the investigated event.

2. Convective systems are generally associated with vertical motion. WRF outputs offers 3D information allowing the generation of vertical cross-section plots or Skew-T diagrams, none of them are shown in the paper. Some graphs and words about this should be added.

Reply: the physical mechanism responsible for the generation of the back-building MCS observed on 25 september 1915 also has been recently explained by Fiori et al. (2017). Taking advantage of the availability of both observational data and modelling results at the micro-α meteorological scale, Fiori et al. (2017) provide insights about the triggering mechanism and the subsequent spatio-temporal evolution of the Genoa 2014 back-building MCS. The major finding is the important effect of a virtual mountain created on the Ligurian sea by the convergence of a cold and dry jet outflowing from the Po valley and a warm and moist low level south-easterly jet within the PBL.

The same mechanism is active also for this case. Let us consider, as an example, the convective flow field at 06UTC on 25 september 1915 (see Figure 3), as predicted by member 1 of the ensemble. Panel A shows the 2 m potential temperature field together with the 10 m horizontal wind vector field: the colder and drier jet outflowing from the Po valley and the warmer and moister air from southern mediterranean sea are evident. Panel B shows, by means of the potential temperature along the cross section corresponding to the green dotted line of Panel A, also the thin potential temperature layer (virtual mountain) in front of the actual Liguria topography. This acts, in agreement with Fiori et al. (2017), to produce the strong convective cells in panel C (updraft velocity above 10 m/s) with the apparent back-building on the western side (less mature and intense cells around 8.4° latitude). The main updraft produces vertical advection of water vapor (panel D), thus resulting in significant production of rainwater (panel E), snow (panel F, significantly advected inland by the upper level south-westerly winds), and graupel (panel G).

This analysis in now included in the revised version of the manuscript.

3. In general the writing style and content is of good quality but the graphs are not at the same level of quality. Fig. 2 has a background hard to see, Fig. 3 has low quality, Fig. 8 is upgradable, etc. (Check the Specific comments).

Reply: we agree on the comments on the figures: the figures of the revised version of the manuscript have been reformat and reorganising according to the suggestions from reviewers.

4. While the convergence line is a very important criteria for dynamics exploration, it hasn't been shown in any figure. Lines 273 and 274 signals the coordinates of this line but a graphical representation would clarify it.

Reply: in the current version of the manuscript, the convergence lines corresponding to members 1, 13, 22 and 37 are highlighted by Figs. 10 and 11. These figures show the 10 m wind fields corresponding to the 4-hour periods with the minimum divergence values in Figure 9. In the revised version of the manuscript, we.

Minor comments

- L113 cites WRF version 2 while the work uses WRF version 3, the correct citation would be thus Skamarock et al. 2008 (NCAR/TN–475+STR)

Reply: we corrected the reference.

- L128 shows a good example in dates using sometimes upper-case and not using this. This is reproduced all over the paper. Consistency in the style should be shown.

Reply: Done; all dates are now upper-case.

- L179 makes reference to Fig. 2b where it's shown 500hPa Geopotential but this is not stated in the text. Please add a comment on this field.

Reply: we corrected the mistake.

- L280 text makes reference to QPF even if this abbreviation hasn't been introduced. Please define it.

Reply: Done.

- L281 addresses Fig. 13 while it should be Fig. 11.

Reply: we corrected the mistake.

- L296 mentions a panel 6 which it's not shown in Fig. 10

Reply: we corrected the mistake.

References

Duda, J. D., & Gallus Jr, W. A. (2013). The Impact of Large-Scale Forcing on Skill of Simulated Convective Initiation and Upscale Evolution with Convection-Allowing Grid Spacings in the WRF. Weather and Forecasting, 28(4), 994-1018.

Fiori, E., L. Ferraris, L. Molini, F. Siccardi, D. Kranzlmueller, and A. Parodi (2016), Triggering and evolution of a deep convective system in the Mediterranean Sea:

modelling and observations at a very fine scale.. Q.J.R. Meteorol. Soc. Accepted Author Manuscript. doi:10.1002/qj.2977.

Han, J., & Pan, H. L. (2011). Revision of convection and vertical diffusion schemes in the NCEP global forecast system. Weather and Forecasting, 26(4), 520-533.

Mass, C. F., Ovens, D., Westrick, K., & Colle, B. A. (2002). Does increasing horizontal resolution produce more skillful forecasts?. Bulletin of the American Meteorological Society, 83(3), 407-430.

Squitieri, B. J., & Gallus Jr, W. A. (2016). WRF Forecasts of Great Plains Nocturnal Low-Level Jet-Driven MCSs. Part II: Differences between Strongly and Weakly Forced Low-Level Jet Environments. Weather and Forecasting, 31(5), 1491-1510.

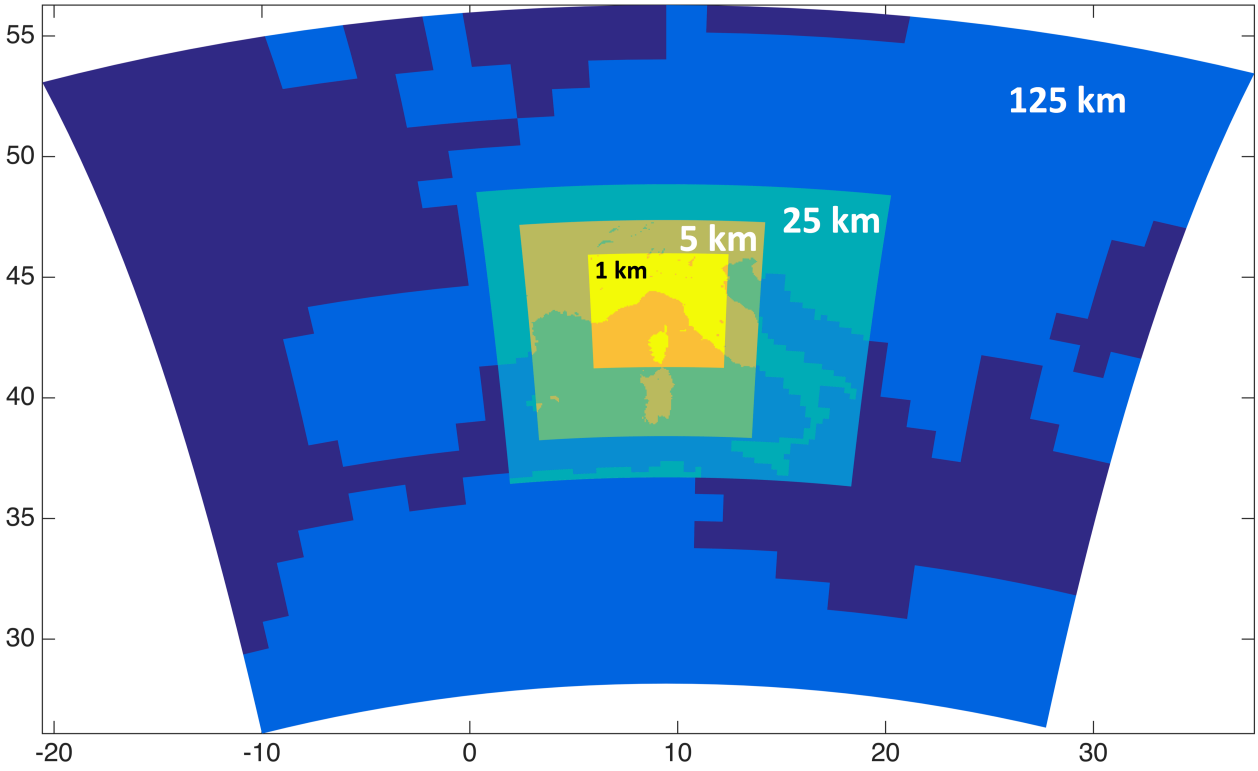

Figure 1: ARF-WRF 4-domains setup.

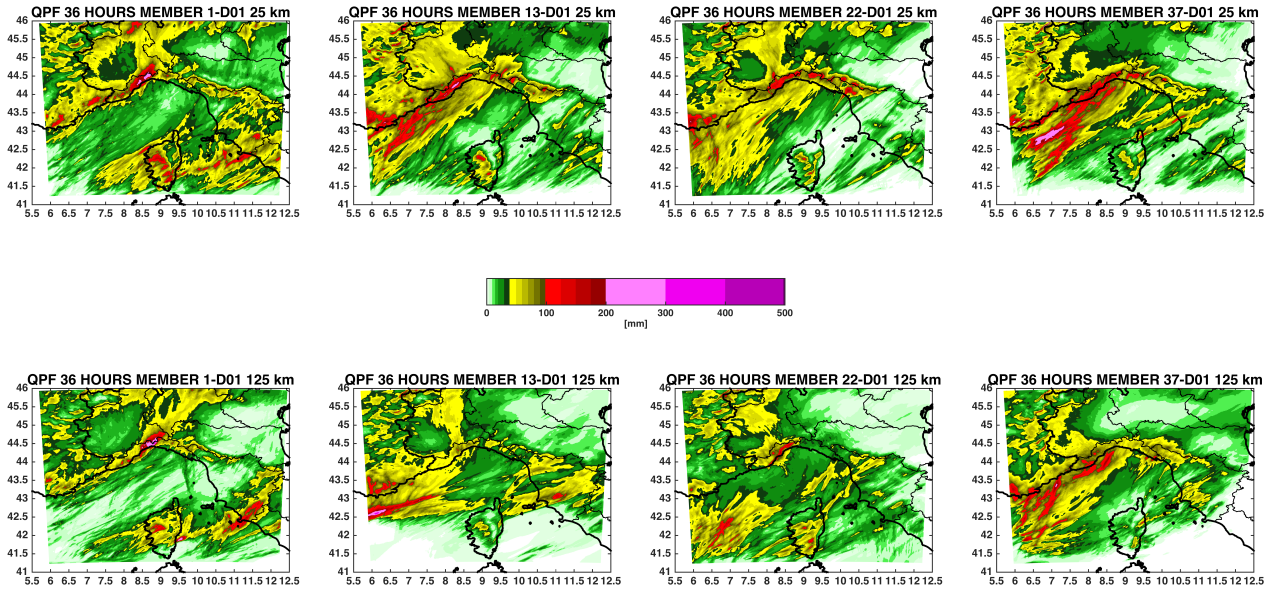

Figure 1: QPF 1 km grid spacing 12UTC 24-09-1915 – 00UTC 26-09-1915 for the ensemble members 1, 13, 22 and 37: first row results corresponding to simulations driven by outermost domain at 25 km grid spacing, second row the same but with outermost domain at 125 km grid spacing.

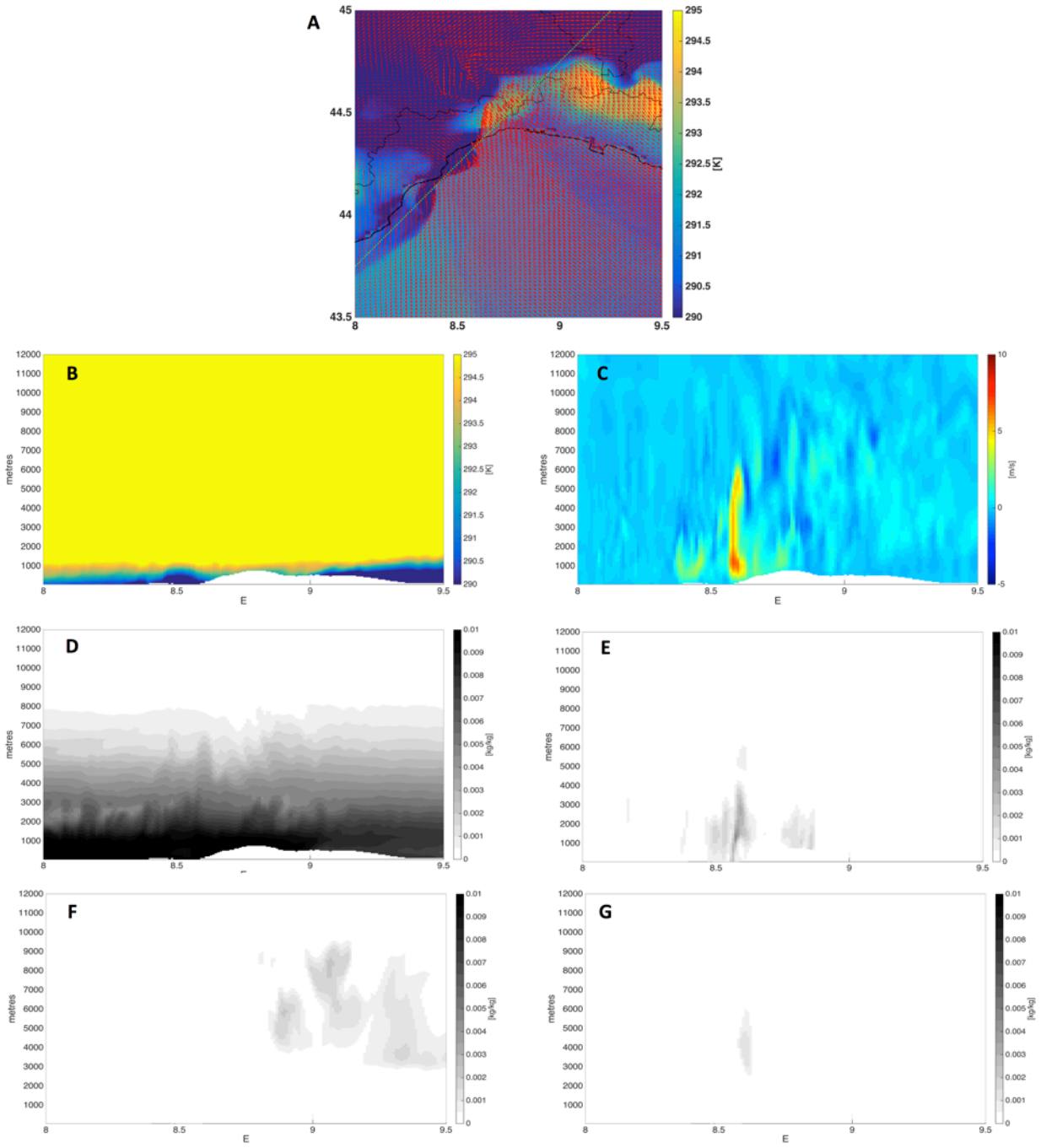

Figure 3: Member 1, 06UTC on 25th September 1915. Panel A shows the 2 m potential temperature field, together with the 10 m horizontal wind vector field. Panels B to G show, instead, potential temperature, vertical velocity, water vapour, rain water, snow, and graupel mixing ratios along the cross section corresponding to the green dotted line shown in panel A.

Ensemble cloud-resolving modelling of a historic back-building mesoscale convective system over Liguria: The San Fruttuoso case of 1915

Antonio Parodi[1], Luca Ferraris[1,2], William Gallus[3], Maurizio Maugeri[4], Luca Molini[1], Franco Siccardi[1], and Giorgio Boni[1,2]

1- CIMA Research Foundation, Savona, Italy
2- Dipartimento di Informatica, Bioingegneria, Robotica e Ingegneria dei Sistemi, University of Genoa, 16145 Genoa, Italy
3- Department of Geological and Atmospheric Sciences, Iowa State University, Ames, Iowa
4- Università degli Studi di Milano, Dipartimento di Fisica, Milan, Italy

Abstract

Highly localized and persistent back-building mesoscale convective systems represent one of the most dangerous flash-flood producing storms in the north-western Mediterranean area. Substantial warming of the Mediterranean Sea in recent decades raises concerns over possible increases in frequency or intensity of these types of events as increased atmospheric temperatures generally support increases in water vapor content. However, analyses of the historical record do not provide a univocal answer, but these are likely affected by a lack of detailed observations for older events.

In the present study, 20th Century Reanalysis Project initial and boundary condition data in ensemble mode are used to address the feasibility of performing cloud-resolving simulations with 1 km horizontal grid spacing of a historic extreme event that occurred over Liguria: The San Fruttuoso case of 1915**.** The proposed approach focuses on the ensemble Weather Research and Forecasting (WRF) model runs that show strong convergence over the Liguria sea, as these runs are the ones most likely to best simulate the event. It is found that these WRF runs generally do show wind and precipitation fields that are consistent with the occurrence of highly localized and persistent back-building mesoscale convective systems, although precipitation peak amounts are underestimated. Systematic small north-westward position errors with regard to the heaviest rain and strongest convergence areas imply that the Reanalysis members may not be adequately representing the amount of cool air over the Po Plain outflowing into the Liguria Sea through the Apennines gap. Regarding the role of historical data sources, this study shows that in addition to Reanalysis products, unconventional data, such as historical meteorological bulletins newspapers and even photographs can be very valuable sources of knowledge in the reconstruction of past extreme events.

1. Introduction

Flash floods are phenomena very common to most Mediterranean coastal cities, accountable for millions of euros of damage and tens to hundreds of victims every year (Gaume et al. 2009). The north-western Mediterranean area is affected by such events in a period usually spanning from late summer (the end of August) to late fall (early December): in this period, the warm waters of the sea, in combination with large-scale meteorological systems coming from the Atlantic Ocean, provide a huge amount of energy, namely latent and sensible heat fluxes, to the atmosphere (Reale et al. 2001, Boni et al. 2006, Pinto et al. 2013). Heavy precipitation is then triggered by the typically very steep topography of the coasts: it is frequent to observe the monthly average rainfall to fall intensely in just a few hours and/or a significant fraction (up to 30-40%) of the yearly average in one day (Parodi et al 2012, Fiori et al. 2014). Obviously, the losses experienced in terms of human lives and economic damage in these very densely populated areas are often dramatic.

Among the flash flood producing storms in the Mediterranean area, a prominent feature is the highly localized and persistent back-building of mesoscale convective systems (MCSs, Schumacher and Johnson 2005, Duffourg et al. 2015, Violante et al. 2016). Such a scenario has been observed often in the last decade, when Liguria (NW Italy) and Southern France have been repeatedly hit by severe floods: 2010 Varazze and Sestri Ponente, 2011 Cinqueterre and Genoa, 2012 Marseille and Isle du Levant, 2014 Genoa and Chiavari, 2015 Nice. As shown in several recent works (Parodi et al. 2012, Rebora et al. 2013, Fiori et al. 2014, Duffourg et al 2015, Silvestro et al. 2015, Cassola et al. 2016, Silvestro et al. 2016), convective cells, embedded in such MCSs, are generated on the sea by the convergence of a warm and moist south-easterly flow and a northerly much colder and drier one. These structures are then advected to the land where the combined action of the aforementioned currents and the topography force them to persist for several hours over a very localized area (e.g. about 100 km^2).

Many flood frequency studies have been carried out, focusing on rainfall regimes and Mediterranean flood seasonality and type (Barriendos et al. 2003, Llasat et al. 2005, Barriendos et al. 2006, Boni et al. 2006, Pinto et al. 2013, Llasat et al. 2014, Toreti et al. 2015). Due to the exploitation of both documentary sources and early measurements, these analyses have been able to go back several centuries, however, their results have been mostly inconclusive regarding changes in frequency of occurrence. Well-defined trends have not been found as usually flood frequency oscillates from period to period with no significant growth, not even in the most recent decades, regardless of the event's duration (a few hours to days).

The same result applies to precipitation extremes and their possible changes over the Mediterranean area in recent decades, studied by several authors, either by empirical or (mainly at-site) extreme value theory approaches (see e.g. Brunetti et al., 2001, 2004, Alpert et al., 2002, Kostopoulou and Jones, 2005, Moberg et al., 2006, Brunet et al., 2007, Kioutsioukis et al., 2010, Rodrigo, 2010, Toreti et al., 2010, van den Besselaar et al., 2013). The temporal tendencies are not fully coherent throughout the region (Ulbrich et al., 2012) and rather conditioned by the specific site, the approach used and the period examined (Brugnara et al., 2012, Brunetti et al., 2012, Maugeri et al., 2015). On the contrary, an increase in precipitation extremes over the Mediterranean area is generally indicated by climate model scenarios (Alpert et al., 2002, Giorgi and Lionello, 2008, Trenberth, 2011).

It is therefore still an open debate whether the frequency of these phenomena is really increasing or if it is merely the perception of both the general public and scientific community. The latter hypothesis is supported by the fact that in the last 10-20 years the observational capabilities have substantially increased. For example, in Italy alone, the remotely automated weather station network has grown to 5000 stations offering an average density of about 1/75 station/km^2 with a 1 to 10-minute sampling rate. At the same time, the national weather radar network reached a fully operational coverage allowing for direct evaluation of the space-time structure of precipitation (Rebora et al. 2013).

Another factor contributing to enhance the perception of an increasing frequency of extreme precipitation and floods is that it has become much easier for weather-related disasters to make it to the news (Pasquaré and Oppizzi 2012, Grasso and Crisci 2016) and therefore to the general public. Moreover, a rapidly growing population and soil consumption increases the exposure of the population to such phenomena (Ward et al. 2013, European Environmental Agency, 2015).

To better investigate whether extreme precipitation and flood frequency are really increasing in the Mediterranean, it is important to improve the exploitation of the information available from past meteorological data. A contribution to this improvement may come from the development of methods that identify which ensemble analyses from projects like the 20th Century Reanalysis Project are able to produce precipitation fields that are reasonably intense and capable of causing extreme floods.

This paper focuses on a case study with the aim of investigating the ability of cloud-resolving grid spacing atmospheric simulations to capture the main features of an event causing a very severe flash flood. These simulations are performed using the Weather Research and Forecasting (WRF, Skamarock et al. 2005) numerical meteorological model forced by an ensemble of reanalysis fields from the 20th Century Reanalysis Project (Compo et al. 2006, Compo et al. 2011). The work is also important to reveal how well fine-scale models can simulate an event for which observations used to initialize the forcing model are extremely sparse (see section 4). One prior work, Michaelis and Lackmann (2013), showed some promising results in the use of WRF for another historical event, the New England Blizzard of 1888, but that event was a midlatitude cyclone driven by dynamics on a larger-scale. More on the windstorm modelling side, Stucki et al. (2015) reconstructed a 1925 high-impact foehn storm in the Swiss Alps.

In this study, the case under investigation was a very intense flash-flood producing event that occurred in 1915 in eastern Liguria (20-25 km east of Genoa, Liguria region capital city), affecting San Fruttuoso, a small hamlet near Portofino, and the coastal cities of Santa Margherita Ligure, Rapallo, and Chiavari (Figure 1). Based on the newspapers of the time and documentary sources, after relatively light rain during the night between September 24th and 25th, on the early morning of September 25th, the area was hit for a few hours (7-11 UTC) by violent rain that triggered widespread flash flooding, and a devastating debris flow. This landslide half-demolished the San Fruttuoso thousand-year old abbey and laid down a thick layer of sand and rocks to form a still existing 20-metre-wide 2-metre-deep beach (Faccini et al. 2008), nowadays a very popular seaside resort. Based both on the observations of the time (wind speed/direction, rainfall, observed lightnings) available for north-western Italy, and on the model simulations, the occurrence of a back-building MCS is suggested.

The paper is organized as follows. In Section 2 the 1915 convective event is presented. Section 3 describes the WRF model setting performed. Results are discussed in Section 4. Conclusions are drawn in Section 5.

2. Meteorological scenario

The synoptic and mesoscale information for this event are available both from the 20th Century Reanalysis Project (Compo et al. 2006, Compo et al. 2011) and from the weather bulletins issued on a daily basis by the Italian Royal Central Office for Meteorology (Regio Ufficio Centrale di Meteorologia e Geodinamica).

The 20th Century Reanalysis Project is an effort led by the Earth System Research Laboratory (ESRL) Physical Sciences Division (PSD) of the National Oceanic and Atmospheric Administration (NOAA) and the Cooperative Institute for Research in Environmental Sciences (CIRES) at the University of Colorado to produce a reanalysis dataset covering the entire twentieth century, assimilating only surface observations of synoptic pressure, monthly sea surface temperature and sea ice distribution. The observations have been assembled through international cooperation under the auspices of the Atmospheric Circulation Reconstructions over the Earth (ACRE) initiative, and working groups of Global Climate Observing System (GCOS) and World Climate Research Program (WCRP). The Project uses an Ensemble Filter data assimilation method, which directly yields each six-hourly analysis as the most likely state of the global atmosphere, and gives also estimates of the uncertainty in that analysis. This dataset provides the first estimates of global tropospheric variability spanning from 1851 to 2012 with a six-hourly temporal resolution and a 2.0° grid spacing. This study adopts 20th Century Reanalysis Project version 2C, which uses the same model as version 2 with new sea ice boundary conditions from the COBE-SST2 (Hirahara et al. 2014), new pentad Simple Ocean Data Assimilation with sparse input (SODAsi.2) sea surface temperature fields (Giese et al. 2016), and additional observations from ISPD version 3.2.9 (Whitaker et al. 2004, Compo et al. 2013, Krueger et al. 2013, Hirahara et al. 2014, Cram et al. 2015).

The weather bulletins issued by the Italian Royal Central Office for Meteorology include weather maps at 7 UTC and 20 UTC and data (sea level pressure, wind (direction and speed), temperature, cloud cover, cloud direction, state of the sea, weather of the past 24 hours and notes) from about 125 Italian stations.

According to the reanalysis fields, the baroclinic circulation over Europe at 6 UTC of September 25th, (i.e. a few hours before the most intense phase of the event) is quite typical for heavy precipitation events over the study area, with an upper-level trough over Great Britain leading to a diffluent flow over the Liguria sea area, in combination with a widespread high pressure block on eastern Europe and southern Russia (Fig. 2a). The diffluent flow over the Liguria sea area is associated with warm air advection at 850 hPa from the southern Mediterranean towards northern-western Mediterranean coastlines (Fig. 2b). Further information is provided by the mean sea level pressure (MSLP) field at the European scale: both the Italian weather map (7 UTC, Fig. 3a) and the reanalysis field (06 UTC, Figs. 2c and 3b) show an elongated trough over the western Mediterranean and a prominent ridge over south-eastern Europe, representing a blocking condition on the large-scale. The pressure gradient between the Gulf of Lyon and the Northern Adriatic Sea is about 12 hPa, according both to fig 3a and 3b. The Italian weather map gives also evidence of a high pressure ridge extending into the Po Valley, which causes a significant surface pressure gradient between the western part of the Po Valley and the Liguria sea (about 3 hpa), as well as between the eastern and the western parts of the Po Valley (about 4 hPa). This high-pressure ridge is present in the reanalysis MSLP field too (06 UTC, Fig. 3b), even though it is much less evident than in the Italian weather map.

On the mesoscale, at 06 UTC, a significant 2-metre temperature difference, around 3-4 °C, is apparent from 20th Century Reanalysis Project fields between the Po Valley and the Liguria sea (Fig. 4a), as well as a significant 2-metre specific humidity gradient (Fig. 4b). The temperature difference is also confirmed by the available observations at 07 UTC provided the Italian Royal Central Office for Meteorology (Fig. 4c).

These mesoscale features represent the necessary ingredients for the generation of a back-building MCS offshore of the Liguria coastline, as observed in the 2010, 2011 and 2014 high impact weather events in this region (Parodi et al. 2012, Rebora et al. 2013, Fiori et al. 2014).

The back-building MCS hypothesis is supported by the 48-hour quantitative precipitation estimates (QPEs) for the period 24th September 07UTC - 26th September 07UTC (Fig. 5). The raingauges (64) contributing to this map have been provided by different datasets such as the European Climate Assessment & Dataset project (Klein Tank et al. 2002, Klok and Klein Tank 2009), the KNMI Climate Explorer dataset (Trouet and Van Oldenborgh 2013), the Italian Meteorological Society (SMI, Auer et al. 2005), the Piedmont Region climatological dataset (Cortemiglia 1999), and the Chiavari Meteorological Observatory (Ansaloni 2006).

The QPE map shows clearly a v-shaped elongated pattern, very similar to the ones observed for the aforementioned events in Liguria. Based on historical information on sub-daily rain rates, it can be estimated that during the most intense phase of the event, the rainfall depths reached up to 400 mm in approximately 4 hours (7-11 UTC on September 25th) in some raingauges (Faccini et al. 2009): as a consequence of this intense and highly localized rainfall the coastal cities of Rapallo, Santa Margherita Ligure, Chiavari and San Fruttuoso suffered very serious damages (Fig. 6), with a death toll around 25-30 people. Interestingly, as in the case of the Genoa 2014 event (Lagasio et al. 2016) a very intense lightning activity was documented by the Italian Royal Central Office for Meteorology (Fig. 7).

3. ARW-WRF model simulations

The model simulations have been performed using the Advanced Research Weather Research and Forecasting Model (hereafter as ARW-WRF, version 3.4.1). Initial and boundary conditions were provided by the 20th Century Reanalysis Project Version version 2c (Compo et al. 2006, Compo et al. 2011) The ARW-WRF model was applied for each of the 56 members of the ensemble provided by the 20th Century Reanalysis Project database.

The ARW-WRF model is configured for this case study based on the results achieved in the ARF-WRF modelling of the Genoa 2011 and Genoa 2014 v-shape convective structures (Fiori et al. 2011, Fiori et al., 2017). Three nested domains, centered on the Liguria region, were used with the outer nest d01 using 25 km horizontal grid spacing (61x55 grid points), the middle nest d02 using 5 km grid spacing (181x201 grid points) and the innermost nest d03 using 1 km grid spacing (526x526 grid points) (Fig. 8 panel a). Panels b-e of Figure 8 provide the comparison between the soil topography over the d03 area, for d01, d02, d03, and native 1 km grid spacing (for numerical stability reasons, given the very large number of ensemble members, soil topography for domain d03 km was interpolated, as in Fiori et al. (2014 and 2017), from soil topography for domain d02).

The benefits of a high number of vertical levels have been demonstrated in Fiori et al. (2014), and thus the same higher number of vertical levels (84) is adopted in this

study. Since the grid-spacing ranges from the regional modelling limit (25 km) down to the cloud resolving one (1 km), two different strategies have been adopted with regard to convection parameterization. For the domain d01 we adopted the new simplified Arakawa–Schubert scheme (Han and Pan 2011) as it is also used by the 20th Century Reanalysis Project with 2.0° grid spacing. Conversely, a completely explicit treatment of convective processes has been carried out on the d02-5 km and d03-1 km domains (Fiori et al., 2014).

The double-Moment Thompson et al. (2008) scheme for microphysical processes has been adopted: this scheme takes into account ice species processes, whose relevance in this case study is confirmed by the intense lightning activity observed during the event, by modelling explicitly the spatio-temporal evolution of the intercept parameter N_i for cloud ice. Furthermore, the Thompson scheme was shown to be the best performing for the Genoa 2011 and Genoa 2014 studies (Fiori et al. 2014 and 2017). With regard to the results in Fiori et al. (2014) about the role of the prescribed number of initial cloud droplets -Nt_c- created upon autoconversion of water vapour to cloud water and directly connected to peak rainfall amounts, a maritime value corresponding to a Nt_c of $25*10^6$ m^{-3} has been adopted.

It is important to highlight that the availability of the 56 members ensemble is a key strength in the present study, which enables estimates of uncertainties associated with dynamical downscaling down to the ARF-WRF d03-1 km domain.

4. Results and discussion

A fundamental ingredient for the occurrence of back-building MCSs is the presence of a persistent and robust convergence line: the availability of a large 1 km ARF-WRF dynamically downscaled ensemble (56 members) allows the exploration of how many members produce such a convergence line over the northern part of the Liguria sea region where most of such MCSs form (Rebora et al. 2013). A convergence line is here classified as persistent and robust if the minimum value of the divergence within the study area is less than $-7*10^{-3}$ s^{-1} for at least 4 hours in a row. The divergence threshold equal to $-7*10^{-3}$ s^{-1} corresponds to the 99.95% percentile of the divergence values computed in every grid point within the region 7.50-10.25E / 43.75-44.50N in Fig. 8 for each ensemble member in the period 12UTC 24th September – 00UTC 26th September (with a 30-minute time resolution).

Using the above threshold, 17 of the 56 ARW-WRF runs exhibit a persistent and robust convergence line in the considered period. In particular, the time series of divergence for four members (1, 13, 22, and 37 respectively) show that the minimum is reached (Fig. 9) at approximately the same time hourly QPF (Quantitative Precipitation Forecast) exceeds 50 mm/h (Fig. 10, panels a-d, and g-l, members 1 and 13, Fig. 11, panels a-d, and g-l, members 22 and 37); the other 13 members are not shown as they behave very similarly. The four representative members exhibit also large QPFs over the whole 36 hours of the simulations (Fig. 10, panels f and n, members 1 and 13, Fig. 11, panels f and n, members 22 and 37), even though significant differences both in the total amount and in the spatial distribution are found. Significant values of the Lightning Potential Index (LPI, Yair et al. 2010), in good agreement with the observations of the Italian Royal Central Office for Meteorology, are shown in Fig. 10 (panels e and m, members 1 and 13) and Fig. 11, (panels e and m, members 22 and 37).

Yet, most of the back-building MCS-producing members are affected by a non-negligible location error (see panels f and n of Figures 10 and 11 for the four selected

members) with respect to the observed daily rainfall map (Fig. 5). This feature is largely due to a predominance of the south-easterly wind component over the north-westerly one (coming from Po Valley), thus pushing the convergence line too north-westwards (red dashed line), close to the western Liguria coastline. This discrepancy is explained by the highly localized spatio-temporal nature of this event, by the comparatively low spatial density of the surface pressure stations assimilated by the 20th Century Reanalysis Project over the western Mediterranean region (Fig. 12) and by the relatively coarse characteristics (2.0° grid spacing, and 6-hourly temporal resolution) of the 20th Century Reanalysis Project forcing initial and boundary conditions data. For instance, the primary wind convergence area over the sea and the inland area affected by the rainfall (6.5-10.5^{o} E / 43.5-45.5^{o} N) is represented by only a few (2-3) 20th Century Reanalysis Project grid points.

To quantitatively examine precipitation errors for each ARW-WRF ensemble member, a bias and mean absolute error (MAE) analysis of the 36 hour (12UTC 24/09 – 00UTC 26/09) QPF versus the 48 hour QPE (07UTC 24/09 – 07UTC 26/09) is undertaken by comparing the available 64 raingauges with the nearest grid points of the d03-1 km. The use of different time periods for QPE and QPF is not an issue as most of the observed precipitation reported for Liguria fell in a time span encompassed in the run time of the simulations. The results (Fig. 13) show that most of the 56 ARF-WRF members have a negative BIAS of roughly 10-40 mm, largely explained by the ensemble widespread underestimation of the extreme rainfall depths over the coastal cities of Santa Margherita Ligure, Rapallo, and Chiavari. The 17 selected members (red markers) show an average BIAS of -22 mm and a MAE of 40 mm, while the remaining 39 members have an average BIAS of -31 mm and a MAE of 42 mm. Also for the 17 selected members, the BIAS is largely explained by the stations mostly affected by the MCS and it reduces to -8 mm when Chiavari, Cervara and S. Margherita Ligure are excluded from the comparison.

Because traditional verification measures (e.g. point-to-point verification measures) applied to QPF are greatly influenced by location errors (Mass et al. 2002), a deeper understanding of QPF performance in the ARF-WRF ensemble is gained by performing object based verification using the Method for Object-based Diagnostic Evaluation (MODE, Davis et al. 2006a, 2006b), intended to reproduce a human analyst's evaluation of the forecast performance. The MODE analysis is performed using a multi-step automated process. A convolution filter is applied to the raw field to identify the objects. When the objects are identified, some attributes regarding geometrical features of the objects (such as location, size, aspect ratio and complexity) and precipitation intensity (percentiles, etc.) are computed. These attributes are used to merge objects within the same forecast/observation field, to match forecast and observed objects and to summarize the performance of the forecast by attribute comparison. Finally, the interest value combines in a total interest function the attributes (the centroid distance, the boundary distance, the convex hull distance, the orientation angle difference, the object area ratio, the intersection divided by the union area ratio, the complexity ratio, and the intensity ratio) computed in the object analysis, providing an indicator of the overall performance of matching and merging between observed and simulated objects. In the present study, the relative weight of each attribute used the default setting in MODE (National Center for Atmospheric Research (NCAR), 2013). The displacement errors including centroid distance and boundary distance were weighted the greatest in the calculation of total interest.

In our experiment we have empirically chosen the convolution disk radius and convolution threshold, so that this choice would recognize precipitation areas (at least roughly 50x50 km or so) similar to what a human would identify. For each ARF-WRF

ensemble member the 36-hour (12UTC 24/09 – 00UTC 26/09) QPF is compared with the 48-hour QPE (07UTC 24/09 – 07UTC 26/09), both bilinearly interpolated to the same 10 km grid. This grid spacing represents a good compromise between the native 1 km ARF-WRF grid spacing and the 40 km average distance between the available 64 raingauges. After a set of experiments, we fixed the value of the convolution radius to one grid point and the threshold of the convoluted field to 75 mm. Twelve members out of the 17 members selected using the minimum divergence criterion show significant values (above 0.8) of the total interest function (Tab. 1). This value is slightly higher than the default one (0.7) used by MODE to match paired objects, in order to restrict our analysis to the best simulated events. Despite the limited observations available in 1915, our ensemble performs relatively well when considering object-based parameters. Specifically, when examining paired observed and modelled clusters, these twelve members demonstrate useful skill for: centroid distance, providing a quantitative sense of spatial displacement of forecast; forecast area/observed area, providing an objective measure of over-or under-prediction of areal extent of the forecasts; forecast intensity 50/observed intensity 50 and forecast intensity 90/observed intensity 90, providing objective measures of median (50th percentile) and near-peak (90th percentile) intensities found in the objects; and the already mentioned total interest, a summary statistic derived from the fuzzy logic engine with user-defined interest maps for all these attributes plus some others (Tab. 1).

Indeed it is impressive that small centroid distance errors averaging only 114 km with a standard displacement of only 62 km are obtained despite the very crude initialization of a 1915 reanalysis case. In a much more recent set of cases, Duda and Gallus (2013) found an average displacement distance (absolute error) of 105 km for initiation of systems. Squitieri and Gallus (2016) show that centroids of forecasted MCSs in their sample of 31 relatively recent events in the United States Central Plains are usually over 100 km or more removed from the centroids of the observed MCSs. Similarly good performance of the ensemble exists for areal coverage, rainfall intensity (although there is a 30-40% underestimate), and overall characteristics of the forecasted objects as implied by the interest value.

Selected members 1, 13, 22 and 37 (Fig. 14) have total interest values above 0.93 (close to 1 is good) and their paired clusters distance, namely the distance between centroids of observed and simulated rain regions, is around 100 km.

The availability of high resolution simulations allows one to gain a deeper understanding of the dynamics of the San Fruttuoso 1915 storm evolution. The physical mechanism responsible for the generation of the back-building mesoscale convective systems in this area has been recently explained by Fiori et al. (2017). Taking advantage of the availability of both observational data and modelling results at the micro-α meteorological scale, Fiori et al. (2017) provide insights about the triggering mechanism and the subsequent spatio-temporal evolution of the Genoa 2014 back-building MCS. The major finding is the important effect of a virtual mountain created on the Ligurian sea by the convergence of a cold and dry jet outflowing from the Po valley and a warm and moist low level south-easterly jet within the planetary boundary layer.
The same mechanism is active also for this case. Let us consider, as an example the convective flow field at 06UTC on 25 September 1915 (see Fig. 15), as predicted by the member 1 of the ensemble. Panel a shows the 2 m potential temperature field together with the 10 m horizontal wind vector field: the colder and drier jet outflowing from the Po Valley and the warmer and moister air from southern mediterranean sea are evident. Panel b shows, by mean of the potential temperature along the cross section corresponding to the green dotted line of Panel a, also the thin potential

391 temperature layer (virtual mountain) in front of the actual Liguria topography. This
392 acts, in agreement with Fiori et al. (2017), for the strong convective cells along the
393 same line in panel c (updraft velocity above 10 m/s) with the apparent back-building
394 on western side (less mature and intense cells around 8.4° latitude). The main updraft
395 produces vertical advection of water vapor (panel d), thus resulting in significant
396 production of rainwater (panel e), snow (panel f, significantly advected inland by the
397 upper level south-westerly winds), and graupel (panel g).
398

399 **5. Conclusions**

400 Highly localized and persistent back-building MCSs represent one of the most
401 dangerous flash-flood producing storms in the north-western Mediterranean area. A
402 historic extreme precipitation event occurring over Liguria on September 1915, which
403 seems to be due to one of these systems, was investigated in this paper both by
404 means of a large collection of observational data and by means of atmospheric
405 simulations performed using the ARF-WRF model forced by an ensemble of reanalysis
406 fields from the 20th Century Reanalysis Project.

407 The results show that the simulated circulation features are consistent with the
408 hypothesis of a highly localized back-building MCS over Liguria sea, and that the ARF-
409 WRF runs -driven by a significant fraction of the members of the 20th Century
410 Reanalysis Project ensemble- produce fields that are in reasonable agreement with
411 the observed data.

412 The proposed approach was to focus only on the ARF-WRF runs showing strong
413 convergence so as to get the best depiction of the event. Thus, we suggest that, when
414 using datasets such as the 20th Century Reanalysis Project, it is important to consider
415 that the physics/dynamics are likely to play a role in the events of interest, and to
416 follow a similar technique to selectively use the Reanalysis ensemble members best
417 displaying the key physics/dynamics of the event. Future work should test further an
418 approach like this one to get a better understanding of how well the same
419 convergence detection approach in regional climate model simulations of past and
420 future climate (e.g. Pieri et al. 2015 at cloud-permitting grid spacing) can quantify
421 possible changes in back-building MCS precipitation processes.
422 On the data collection side, this study showed that in addition to the use of Reanalysis
423 products, other sources of data, such as newspapers, photographs, and historical
424 meteorological bulletins can be essential sources of knowledge. Focusing on historical
425 meteorological bulletins, future work on this particular case and similar ones occurring
426 along the north-western Mediterranean coastline will explore the use of bogus
427 observations or other preprocessing techniques to alter lower tropospheric conditions
428 at model initialization time to better match actual observations, which may result in a
429 better location of the convergence line and consequently simulation of the
430 precipitation event.
431

432 **6. Acknowledgments**

433 This work was supported by the Italian Civil Protection Department and by the
434 Regione Liguria. The ground based observations were provided by Italian Civil
435 Protection Department and the Ligurian Environmental Agency. The raingauge data
436 were courtesy of the European Climate Assessment & Dataset project, the KNMI
437 Climate Explorer dataset, the Italian Meteorological Society, Piedmont Region
438 climatological dataset, and the Chiavari Meteorological Observatory. Antonio Parodi
439 would like also to acknowledge the support of the FP7 DRIHM (Distributed Research
440 Infrastructure for Hydro-Meteorology, 2011-2015) project (contract number 283568).

Thanks are due to the CINECA, where the numerical simulations were performed on the Galileo System, Project-ID: SCENE. W. Gallus appreciates the opportunity for a research visit at the University of Milan.

7. References

Alpert, P., Ben-Gai, T., Baharad, A., Benjamini, Y., Yekutieli, D., Colacino, M., Diodato, L., Ramis, C., Homar, V., Romero, R., Michaelides, S., & Manes, A. (2002). The paradoxical increase of Mediterranean extreme daily rainfall in spite of decrease in total values. Geophys. Res. Lett., 29(11).

Ansaloni, A. (2006). The Observatory at Chiavari, Italy: its history and museum. Weather, 61(10), 283-285.

Auer, I., Boehm, R., Jurkovic, A., Orlik, A., Potzmann, R., Schoener, W., Ungersboeck, M., Brunetti, M., Nanni, T., Maugeri, M., Briffa, K., Jones, P., Efthymiadis, D., Mestre, O., Moisseline, J.M., Begert, M., Brazdil, R., Bochnicek, O., Cegnar, T., Garjic-Capka, M., Zaninovic, K., Majstorovic, Z., Szalai, S., Szentimery, T., & Mercalli, L. (2005). A new instrumental Precipitation Dataset for the Greater Alpine Region for the period 1800-2002. Int. J. Climatol., 25(2), 139-166.

Barriendos, M., Coeur, D., Lang, M., Llasat, M. C., Naulet, R., Lemaître, D., & Barrera, A. (2003). Stationarity analysis of historical flood series in France and Spain (14th–20th centuries). Natural Hazards and Earth System Science, 3(6), 583-592.

Barriendos, M., & Rodrigo, F. S. (2006). Study of historical flood events on Spanish rivers using documentary data. Hydrological Sciences Journal, 51(5), 765-783.

Boni, G., Parodi, A., & Rudari, R. (2006). Extreme rainfall events: Learning from raingauge time series. Journal of hydrology, 327(3), 304-314.

Brugnara, Y., Brunetti, M., Maugeri, M., Nanni, T., & Simolo, C. (2012). High-resolution analysis of daily precipitation trends in the central Alps over the last century. International Journal of Climatology, 32(9), 1406-1422.

Brunet, M., Jones, P. D., Sigró, J., Saladié, O., Aguilar, E., Moberg, A., Della-Marta, P.M., Lister, D., Walther, A., & López, D. (2007). Temporal and spatial temperature variability and change over Spain during 1850–2005. Journal of Geophysical Research: Atmospheres, 112(D12).

Brunetti, M., Maugeri, M., & Nanni, T. (2001). Changes in total precipitation, rainy days and extreme events in northeastern Italy. International Journal of Climatology, 21(7), 861-871.

Brunetti, M., Buffoni, L., Mangianti, F., Maugeri, M., & Nanni, T. (2004). Temperature, precipitation and extreme events during the last century in Italy. Global and planetary change, 40(1), 141-149.

Brunetti, M., Caloiero, T., Coscarelli, R., Gullà, G., Nanni, T., & Simolo, C. (2012). Precipitation variability and change in the Calabria region (Italy) from a high resolution daily dataset. International Journal of Climatology, 32(1), 57-73.

Cassola, F., Ferrari, F., Mazzino, A., & Miglietta, M. M. (2016). The role of the sea on the flash floods events over Liguria (northwestern Italy). Geophysical Research Letters, 43(7), 3534-3542.

Compo, G. P., Whitaker, J. S., & Sardeshmukh, P. D. (2006). Feasibility of a 100-year reanalysis using only surface pressure data. Bulletin of the American Meteorological Society, 87(2), 175-190.

Compo, G.P., Whitaker, J.S., Sardeshmukh, P.D., Matsui, N., Allan, R.J., Yin, X., Gleason Jr, B.E, Vose, R.S., Rutledge, G., Bessemoulin, P., Brönnimann, S., Brunet, M., Crouthamel, R.I., Grant, A.N., Groisman, P.Y., Jones, P.D., Kruk, M., Kruger, A.C., Marshall, G.J., Maugeri, M., Mok, H.Y., Nordli, Ø., Ross, T.F., Trigo, R.M., Wang, X.L., Woodruff, S.D., & Worley, S.J., (2011). The twentieth century reanalysis project. Quarterly Journal of the Royal Meteorological Society, 137(654), 1-28.

Compo, G. P., Sardeshmukh, P. D., Whitaker, J. S., Brohan, P., Jones, P. D., & McColl, C. (2013). Independent confirmation of global land warming without the use of station temperatures. *Geophysical Research Letters*, *40*(12), 3170-3174.

Cortemiglia, G. C. (1999). Serie climatiche ultracentenarie (con allegato CD ROM). Collana Studi Climatologici in Piemonte, Regione Piemonte, 3, 1-92.

Cram, T.A., Compo, G.P., Yin, X., Allan, R.J., McColl, C., Vose, R.S., Whitaker, J.S., Matsui, N., Ashcroft, l., Auchmann, R., Bessemoulin, P., Brandsma, T., Brohan, P., Brunet, M., Comeaux, J., Crouthamel, R., Gleason B.E. Jr, Groisman, P.Y., Hersbach, H., Jones, P.D., Jónsson, T., Jourdain, S., Kelly, G., Knapp, K.R., Kruger, A., Kubota, H., Lentini, G., Lorrey, A., Lott, N., Lubker, S.J., Luterbacher, J., Marshall, G.J., Maugeri, M., Mock, C.J., Mok, H.J., Nordli, O., Rodwell, M.J., Ross, T.F., Schuster, D., Srnec, L., Valente, M.A., Vizi, Z., Wang, X.L., Westcott, N., Woollen, J.S., & Worley, S.J. (2015). The international surface pressure databank version 2. Geoscience Data Journal, 2(1), 31-46.

Davis, C., B. Brown, & R. Bullock, 2006a: Object-based verification of precipitation forecasts. Part I: Methods and application to mesoscale rain areas. Mon. Wea. Rev., 134, 1772–1784.

Davis, C., B. Brown, & R. Bullock, 2006b: Object-based verification of precipitation forecasts. Part II: Application to convective rain systems. Mon. Wea. Rev., 134, 1785–1795.

Duda, J. D., & Gallus Jr, W. A., 2013: The Impact of Large-Scale Forcing on Skill of Simulated Convective Initiation and Upscale Evolution with Convection-Allowing Grid Spacings in the WRF*. Weather and Forecasting, 28(4), 994-1018.

Duffourg, F., Nuissier, O., Ducrocq, V., Flamant, C., Chazette, P., Delanoe, J., Doerenbecher, A., Fourrié, N., Di Girolamo, P., Lac, C., Legain, D., Martinet, M., Said, F., & Bock, O. ... & Legain, D. (2015). Offshore deep convection initiation and maintenance during I0P16a Offshore deep convection initiation and maintenance during HyMeX IOP 16a heavy precipitation event. Quarterly Journal of the Royal Meteorological Society. 142: 259–274.

European Environmental Agency (2015), SOER 2015 — The European environment — state and outlook 2015 A comprehensive assessment of the European environment's state, trends and prospects, in a global context.

Faccini, F., Piccazzo, M., & Robbiano, A. (2009). Natural hazards in San Fruttuoso of Camogli (Portofino Park, Italy): a case study of a debris flow in a coastal environment. Bollettino della Societa Geologica Italiana, 128(3), 641-654.

Fiori, E., Comellas, A., Molini, L., Rebora, N., Siccardi, F., Gochis, D. J., Tanelli, S., & Parodi, A. (2014). Analysis and hindcast simulations of an extreme rainfall event in the Mediterranean area: The Genoa 2011 case. Atmospheric Research, 138, 13-29.

Fiori, E., Ferraris, L., Molini, L., Siccardi, F., Kranzlmueller, D. & Parodi, A. (2017), Triggering and evolution of a deep convective system in the Mediterranean Sea: modelling and observations at a very fine scale. Q.J.R. Meteorol. Soc. doi:10.1002/qj.2977.

Gaume, E., Bain, V., Bernardara, P., Newinger, O., Barbuc, M., Bateman, A., Blaškovicová, L., Blöschl, G., Borga, M., Dumitrescu, A., Daliakopoulos, J., Garcia, J., Irimescu, A., Kohnova, S., Koutroulis, A., Marchi, L., Matreata, S., Medina, V., Preciso, E., Sempere-Torres, D., Stancalie, G., Szolgay, J., Tsanis, J., Velascom, D., & Viglione, A. (2009). A compilation of data on European flash floods. Journal of Hydrology, 367(1), 70-78.

Giese, B. S., Seidel, H. F., Compo, G. P., & Sardeshmukh, P. D. (2016). An ensemble of ocean reanalyses for 1815–2013 with sparse observational input. Journal of Geophysical Research: Oceans.

Giorgi, F., & Lionello, P. (2008). Climate change projections for the Mediterranean region. Global and Planetary Change, 63(2), 90-104.

Grasso, V., & Crisci, A. (2016). Codified hashtags for weather warning on Twitter: an Italian case study. PLoS currents, 8.

Han, J., & Pan, H. L. (2011). Revision of convection and vertical diffusion schemes in the NCEP global forecast system. *Weather and Forecasting*, *26*(4), 520-533.

Hirahara, S., Ishii, M., & Fukuda, Y. (2014). Centennial-scale sea surface temperature analysis and its uncertainty. *Journal of Climate*, *27*(1), 57-75.

Klein Tank, A.M.G., Wijngaard, J.B., Können, G.P., Böhm, R., Demarée, G., Gocheva, A., Mileta M., Pashiardis, S., Hejkrlik, L., Kern-Hansen, C., Heino, R., Bessemoulin, P., Müller-Westmeier, G., Tzanakou, M., Szalai1, S., Pálsdóttir, T., Fitzgerald, D., Rubin, S., Capaldo, M., Maugeri, M., Leitass, A., Bukantis, A., Aberfeld, R., van Engelen, A.F.V., Forland, E., Mietus, M., Coelho, F., Mares, C., Razuvaev, V., Nieplova, E., Cegnar, T., Antonio López, J., Dahlström, B., Moberg, A., Kirchhofer, W., Ceylan, A., Pachaliuk, O., Alexander, L.V., & Petrovic, P. (2002). Daily dataset of 20th - century surface air temperature and precipitation series for the European Climate Assessment. International journal of climatology, 22(12), 1441-1453.

Klok, E. J., & Klein Tank, A. M. G. (2009). Updated and extended European dataset of daily climate observations. International Journal of Climatology, 29(8), 1182-1191.

595 Kioutsioukis, I., Melas, D., & Zerefos, C. (2010). Statistical assessment of changes in
596 climate extremes over Greece (1955–2002). International Journal of Climatology,
597 30(11), 1723-1737.
598
599 Kostopoulou, E., & Jones, P. D. (2005). Assessment of climate extremes in the
600 Eastern Mediterranean. Meteorology and Atmospheric Physics, 89(1-4), 69-85.
601
602 Krueger, O., Schenk, F., Feser, F., & Weisse, R. (2013). Inconsistencies between long-
603 term trends in storminess derived from the 20CR reanalysis and observations. *Journal
604 of Climate*, *26*(3), 868-874.
605
606 Lagasio, M., Fiori, E., Procopio, R., & Parodi, A. (2016). Lightning flash activity indices
607 as forecasting tool of high impact weather events over complex topography: The
608 Genoa 2014 critical case, in preparation.
609
610 Llasat, M. C., Barriendos, M., Barrera, A., & Rigo, T. (2005). Floods in Catalonia (NE
611 Spain) since the 14th century. Climatological and meteorological aspects from
612 historical documentary sources and old instrumental records. Journal of Hydrology,
613 313(1), 32-47.
614
615 Llasat, M. C., Marcos, R., Llasat-Botija, M., Gilabert, J., Turco, M., & Quintana-Seguí,
616 P. (2014). Flash flood evolution in North-Western Mediterranean. Atmospheric
617 Research, 149, 230-243.
618
619 Maugeri, M., Brunetti, M., Garzoglio, M., & Simolo, C. (2015). High-resolution analysis
620 of 1 day extreme precipitation in Sicily. Natural Hazards and Earth System Science,
621 15(10), 2347-2358.
622
623 Mass, C. F., Ovens, D., Westrick, K., & Colle, B. A. (2002). Does increasing horizontal
624 resolution produce more skillful forecasts?. Bulletin of the American Meteorological
625 Society, 83(3), 407-430.
626
627 Michaelis, A. C., & Lackmann, G. M. (2013), Numerical modelling of a historic storm:
628 Simulating the Blizzard of 1888. Geophysical Res. Letters, 40, 4092-4097.
629
630 Moberg, A., Jones, P.D., Lister, D., Alexander, W., Brunet, M., Jacobeit, J., Alexander,
631 L.V., Della-Marta, P.M., Luterbacher, J., Yiou, P., Chen, D., Klein Tank, A.M.G.,
632 Saladié, O., Sigró, J., Aguilar, E., Alexandersson, H., Almarza, C., Auer, I., Barriendos,
633 M., Begert, M., Bergström, H., Böhm, R., Butler, C.J., Caesar, J., Drebs, A., Founda,
634 D., Gerstengarbe, F.W., Micela, G., Maugeri, M., Österle, H., Pandzic, K., Petrakis, M.,
635 Srnec, L., Tolasz, R., Tuomenvirta, H., Werner, P.C., Linderholm, H., Philipp, A.,
636 Wanner, H., & Xoplaki, E. (2006). Indices for daily temperature and precipitation
637 extremes in Europe analyzed for the period 1901–2000. Journal of Geophysical
638 Research: Atmospheres, 111, D22106.
639
640 National Center for Atmospheric Research (NCAR) (2013). Model Evaluation Tools
641 version 4.1 (METv4.1): User's guide 4.1. Developmental Testbed Center Rep., 226 pp.
642 [Available online at
643 http://www.dtcenter.org/met/users/docs/users_guide/MET_Users_Guide_v4.1.pdf.]
644
645 Parodi, A., Boni, G., Ferraris, L., Siccardi, F., Pagliara, P., Trovatore, E., Foufoula-
646 Georgiou, E., & Kranzlmueller, D. (2012). The "perfect storm": From across the

Atlantic to the hills of Genoa. Eos, Transactions American Geophysical Union, 93(24), 225-226.

Pasquaré, F. A., & Oppizzi, P. (2012). How do the media affect public perception of climate change and geohazards? An Italian case study. Global and Planetary Change, 90, 152-157.

Pieri, A. B., von Hardenberg, J., Parodi, A., & Provenzale, A. (2015). Sensitivity of Precipitation Statistics to Resolution, Microphysics, and Convective Parameterization: A Case Study with the High-Resolution WRF Climate Model over Europe. Journal of Hydrometeorology, 16(4), 1857-1872.

Pinto, J. G., Ulbrich, S., Parodi, A., Rudari, R., Boni, G., & Ulbrich, U. (2013). Identification and ranking of extraordinary rainfall events over Northwest Italy: The role of Atlantic moisture. Journal of Geophysical Research: Atmospheres, 118(5), 2085-2097.

Reale, O., Feudale, L., & Turato, B. (2001). Evaporative moisture sources during a sequence of floods in the Mediterranean region. Geophysical research letters, 28(10), 2085-2088.

Rebora, N., Molini, L., Casella, E., Comellas, A., Fiori, E., Pignone, F., Siccardi, F., Silvestro, F., Tanelli, S., & Parodi, A. (2013). Extreme rainfall in the mediterranean: what can we learn from observations?. Journal of Hydrometeorology, 14(3), 906-922.

Rodrigo, F. S. (2010). Changes in the probability of extreme daily precipitation observed from 1951 to 2002 in the Iberian Peninsula. International Journal of Climatology, 30(10), 1512-1525.

Schumacher, R. S., & Johnson, R. H. (2005). Organization and environmental properties of extreme-rain-producing mesoscale convective systems. Monthly weather review, 133(4), 961-976.

Silvestro, F., Rebora, N., Giannoni, F., Cavallo, A., & Ferraris, L. (2015). The flash flood of the Bisagno Creek on 9th October 2014: An "unfortunate" combination of spatial and temporal scales. Journal of Hydrology.

Silvestro, F., Rebora, N., Rossi, L., Dolia, D., Gabellani, S., Pignone, F., Trasforini, E., Rudari, R., De Angeli, S., & Masciulli, C. (2016). What if the 25 October 2011 event that struck Cinque Terre (Liguria) had happened in Genoa, Italy? Flooding scenarios, hazard mapping and damage estimation. Natural Hazards and Earth System Sciences, 16(8), 1737-1753.

Skamarock, W. C., Klemp, J. B., Dudhia, J., Gill, D. O., Barker, D. M., Duda, M.G., Xiang-Yu, Wang, W., & Powers, J. G. (2008). A Description of the Advanced Research WRF Version 3 (No. NCAR/TN–475+STR). National Center for Atmospheric Research Boulder, Mesoscale and Microscale Meteorology Division.

Squitieri, B. J., & Gallus Jr, W. A. (2016). WRF Forecasts of Great Plains Nocturnal Low-Level Jet-Driven MCSs. Part II: Differences between Strongly and Weakly Forced Low-Level Jet Environments. Weather and Forecasting, 31(5), 1491-1510.

699 Stucki, P., Brönnimann, S., Martius, O., Welker, C., Rickli, R., Dierer, S., Bresch, D.N,
700 Compo, G.P. & Sardeshmukh, P. D. (2015). Dynamical downscaling and loss modeling
701 for the reconstruction of historical weather extremes and their impacts: a severe
702 Foehn storm in 1925. Bulletin of the American Meteorological Society, 96(8), 1233-
703 1241.
704
705 Thompson, G., Field, P. R., Rasmussen, R. M., & Hall, W. D. (2008). Explicit forecasts
706 of winter precipitation using an improved bulk microphysics scheme. Part II:
707 Implementation of a new snow parameterization. *Monthly Weather Review*, *136*(12),
708 5095-5115.
709
710 Toreti, A., Xoplaki, E., Maraun, D., Kuglitsch, F. G., Wanner, H., & Luterbacher, J.
711 (2010). Characterisation of extreme winter precipitation in Mediterranean coastal sites
712 and associated anomalous atmospheric circulation patterns. Nat. Hazards Earth Syst.
713 Sci, 10(5), 1037-1050.
714
715 Toreti, A., Giannakaki, P., & Martius, O. (2015). Precipitation extremes in the
716 Mediterranean region and associated upper-level synoptic-scale flow structures.
717 Climate Dynamics, 1-17.
718
719 Trenberth, K. E. (2011). Changes in precipitation with climate change. Climate
720 Research, 47(1), 123.
721
722 Trouet, V., & Van Oldenborgh, G. J. (2013). KNMI Climate Explorer: a web-based
723 research tool for high-resolution paleoclimatology. Tree-Ring Research, 69(1), 3-13.
724
725 Ward, P. J., Jongman, B., Weiland, F. S., Bouwman, A., van Beek, R., Bierkens, M. F.
726 P., Ligtvoet, W., & Winsemius, H. C. (2013). Assessing flood risk at the global scale:
727 model setup, results, and sensitivity. Environmental research letters, 8(4), 044019.
728
729 Whitaker, J. S., Compo, G. P., Wei, X., & Hamill, T. M. (2004). Reanalysis without
730 radiosondes using ensemble data assimilation. Monthly Weather Review, 132(5),
731 1190-1200.
732
733 Ulbrich, U., Lionello, P., Belušić, D., Jacobeit, J., Knippertz, P., Kuglitsch, F. G.,
734 Leckebusch, G.C., Luterbacher, J., Maugeri, M., Maheras, P., Nissen, K.M., Pavan, V.,
735 Pinto, J.G., Saaroni, H., Seubert, S., Toreti, A., Xoplaki, E., & Ziv, B. (2012). Climate
736 of the Mediterranean: synoptic patterns, temperature, precipitation, winds, and their
737 extremes. In The Climate of the Mediterranean Region-From the Past to the Future.
738 Elsevier, London.
739
740 Van den Besselaar, E. J. M., Klein Tank, A. M. G., & Buishand, T. A. (2013). Trends in
741 European precipitation extremes over 1951–2010. International Journal of
742 Climatology, 33(12), 2682-2689.
743
744 Violante, C., Braca, G., Esposito, E., & Tranfaglia, G. (2016). The 9 September 2010
745 torrential rain and flash flood in the Dragone catchment, Atrani, Amalfi Coast
746 (southern Italy). Natural Hazards and Earth System Sciences, 16(2), 333-348
747
748 Yair, Y., Lynn, B., Price, C., Kotroni, V., Lagouvardos, K., Morin, E., Mugnai, A., &
749 Llasat, M.d.C. (2010). Predicting the potential for lightning activity in Mediterranean

storms based on the Weather Research and Forecasting (WRF) model dynamic and microphysical fields. Journal of Geophysical Research: Atmospheres, 115, D04205.

Tables and table captions

Parameter	Average	Standard deviation
PAIRED CENTROID DISTANCE (km)	114	62
FCST AREA/OBS AREA	1.10	0.90
FCST INT 50/OBS INT 50	0.73	0.06
FCST INT 90/OBS INT 90	0.62	0.11
TOTAL INTEREST	0.88	0.09

Table 1: Clusters pairs statistics for the 12 members out of 17, showing significant values (above 0.8) of the total interest function.

Figures and figure captions

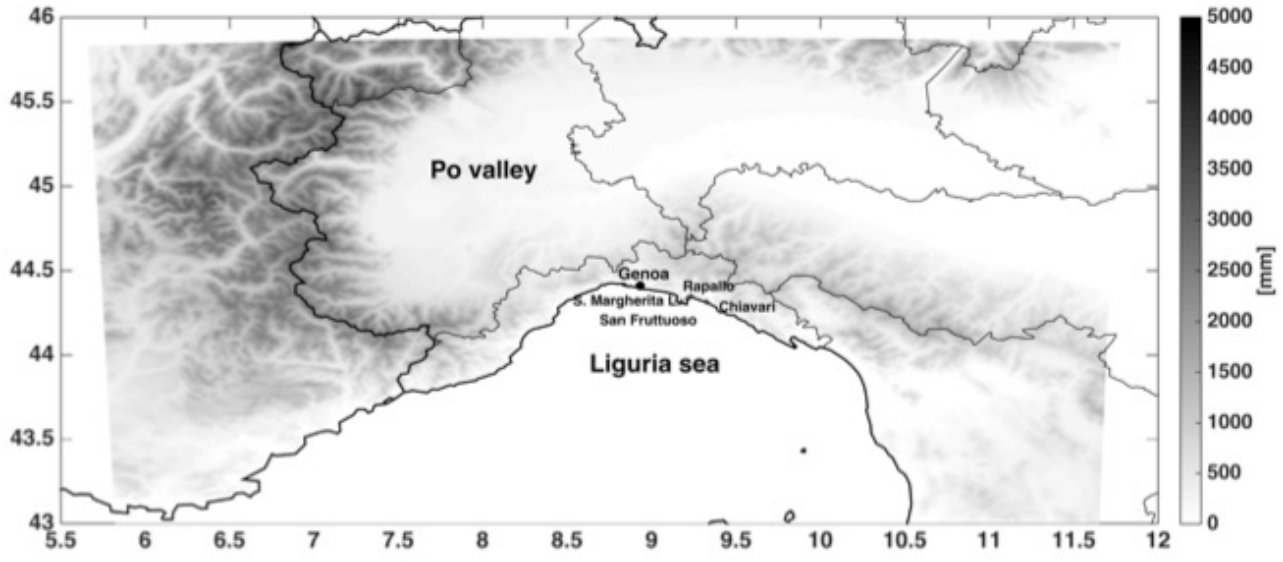

Figure 1: Study region and Liguria coastal cities affected by the September 1915 event.

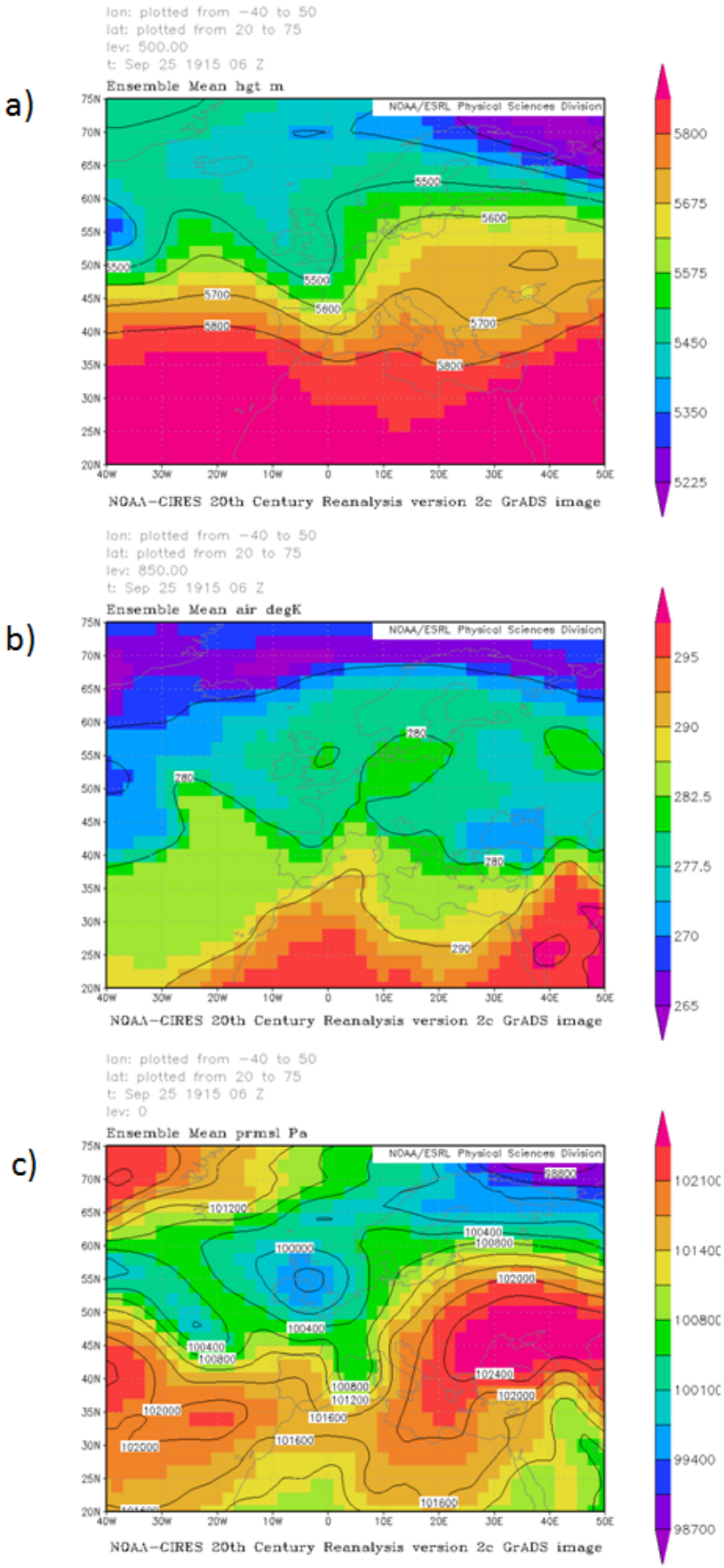

Figure 2: a) 500 hPa geopotential, b) 850 hPa temperature, and c) sea level pressure on 25th September, 1915 06UTC (20th Century Reanalysis Project mean fields over the 56 ensemble members).

a)

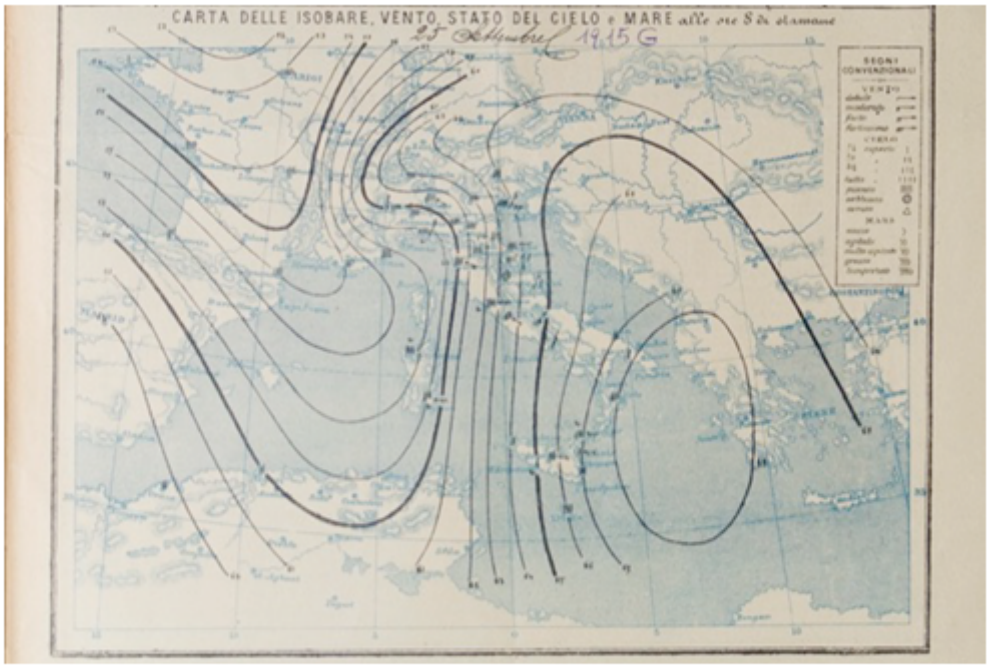

b)

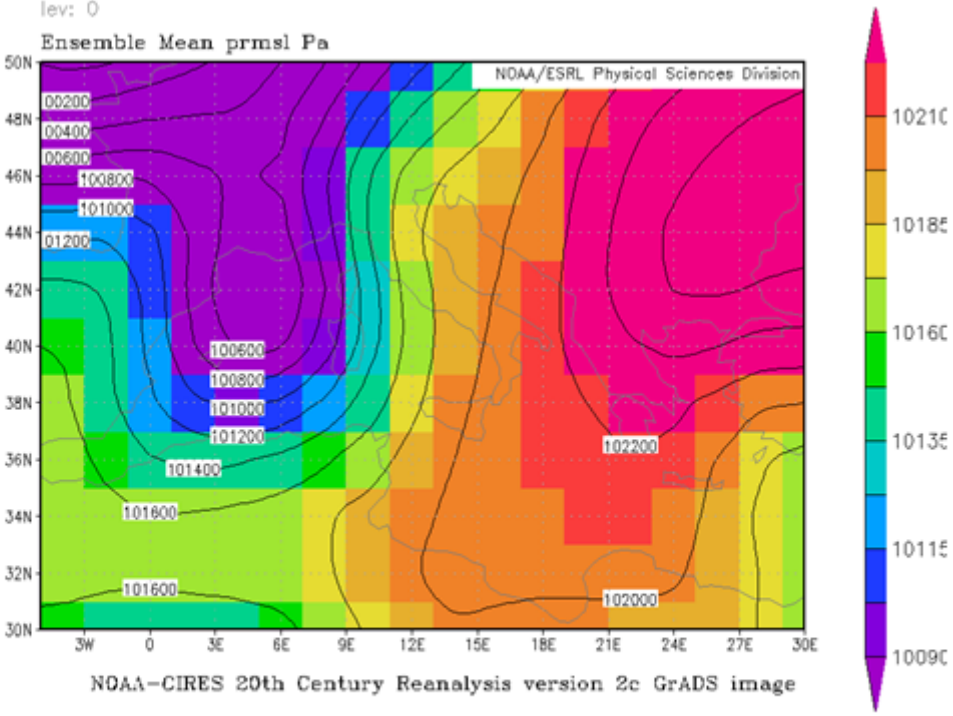

Figure 3: a) see level pressure isobars on 25th September 1915 at 07UTC, as provided by the Italian Royal Meteorological Service. b) the same field as in figure 2c, but over the same area of the map in figure 3a.

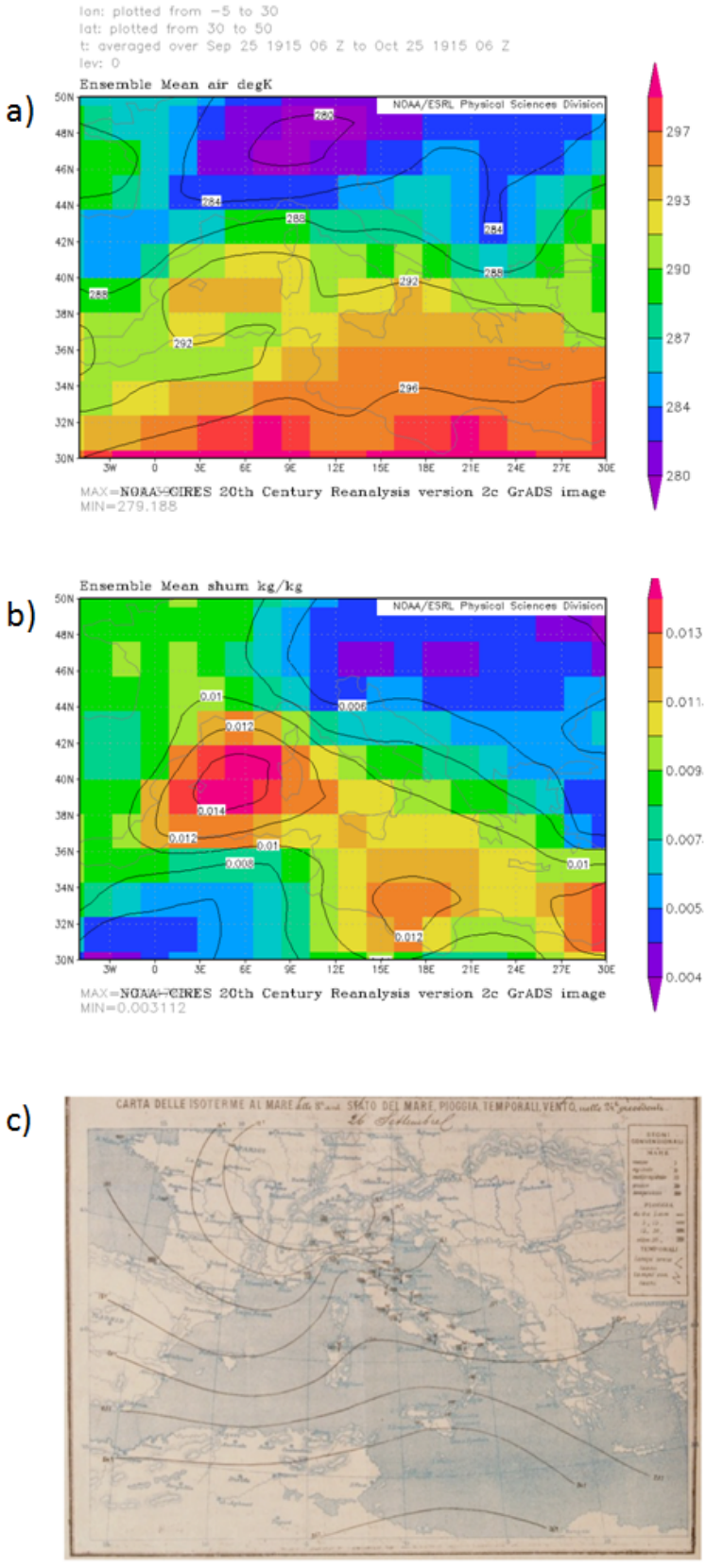

774

775 Figure 4: a) 2 m temperature and b) 2 m specific humidity on 25th September 1915
776 (06 UTC) over the study region. (20th Century Reanalysis mean fields over the 56
777 ensemble members), c) surface temperature isotherms on 25th September 1915
778 (07UTC), as provided by the Italian Royal Meteorological Service.

779

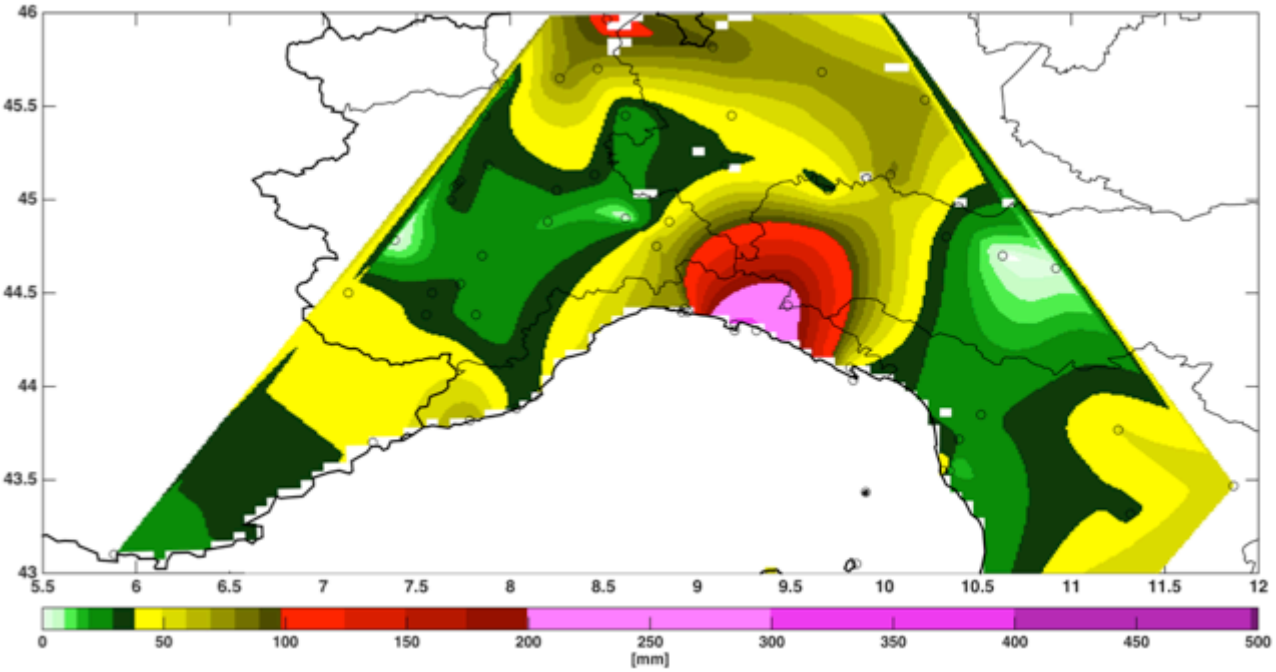

Figure 5: quantitative precipitation estimates (QPE) for 24th September 07UTC - 26th September 1915 07UTC.

790

791
792
793 Figure 6: Rapallo flash-flood impacts on 25th September 1915 (Courtesy of real estate
794 Agency Bozzo in Camogli).
795
796
797

Figure 7: thunderstorms and lightning activity reports (red circle) on 25th September 1915, as provided by the Italian Royal Meteorological Service.

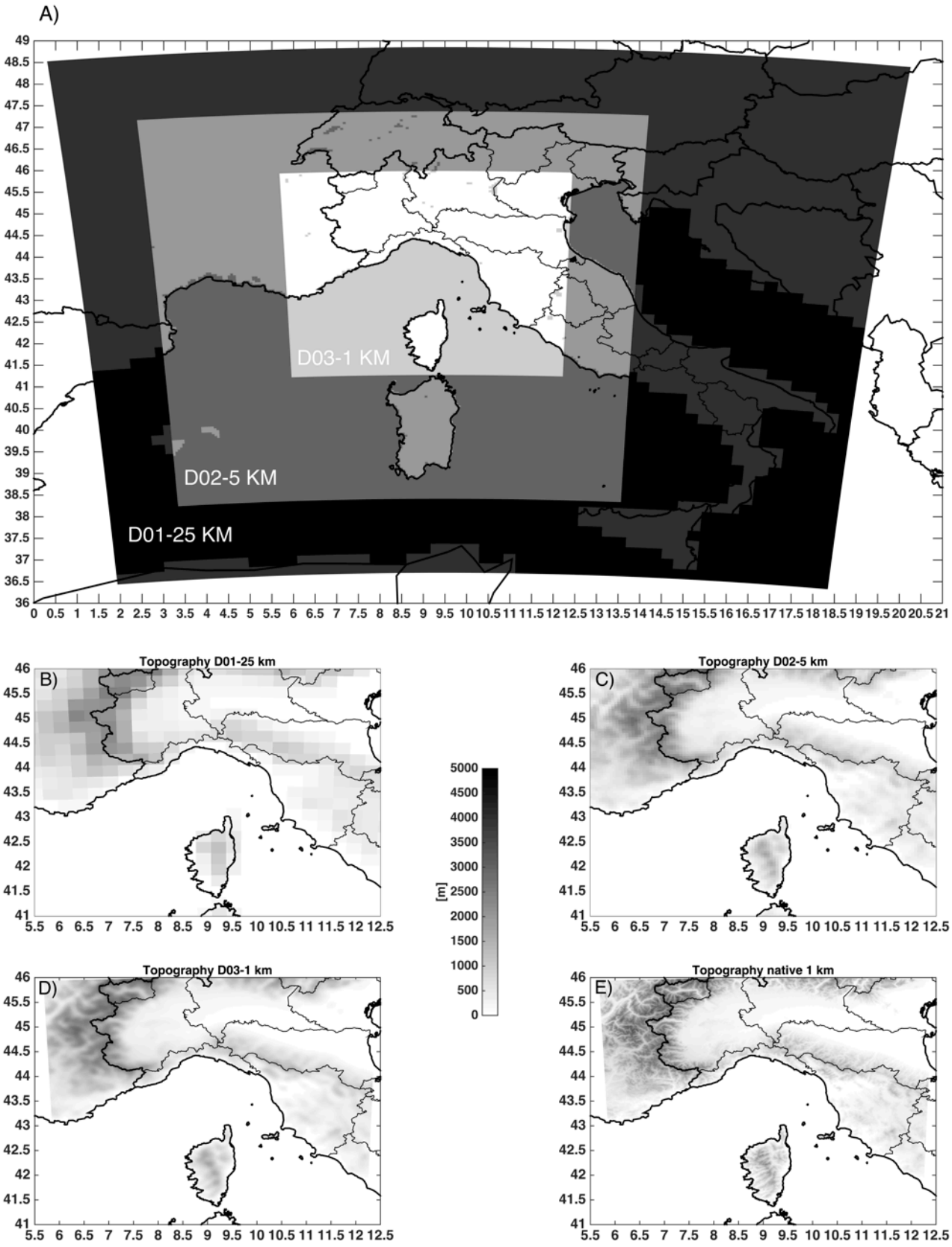

Figure 8: Panel a: domains for the numerical simulations of the Genoa 1915 event, d01 (Δ=25 km), d02 (Δ=5 km) and d03 (Δ=1 km). Panels b-e comparison between the topography over the d03 area, for d01, d02, d03, and native 1 km grid spacing.

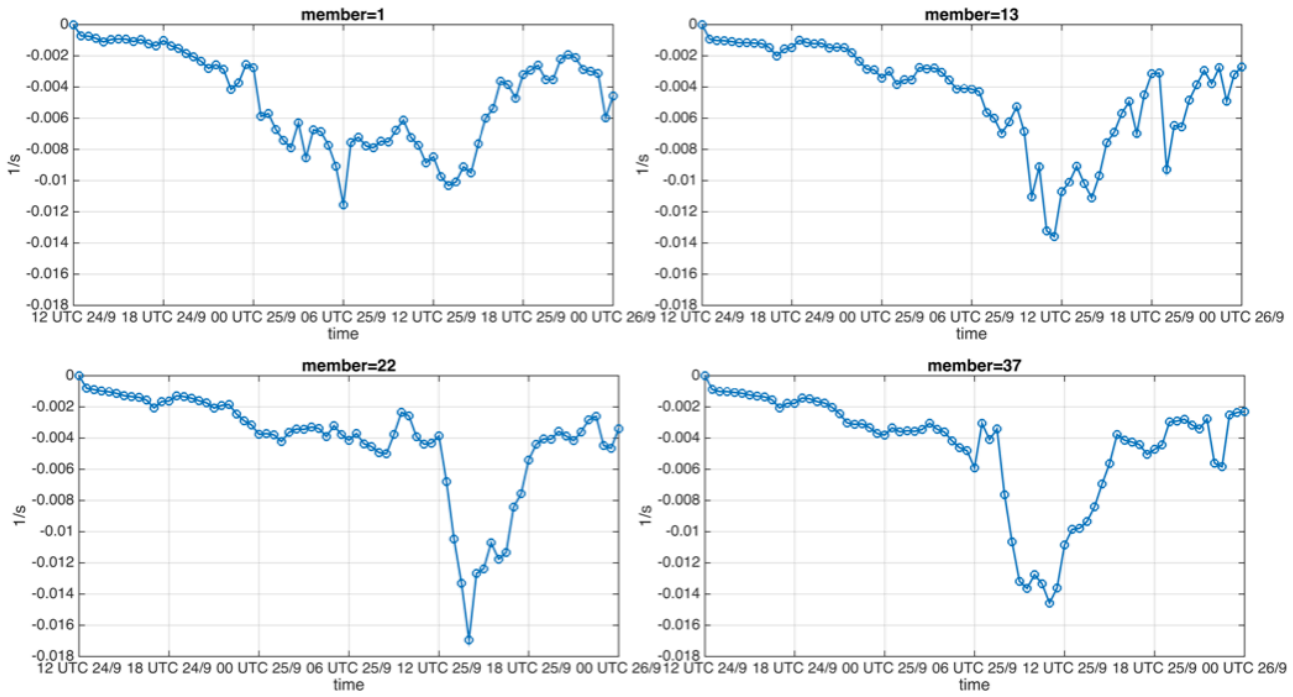

Figure 9: minimum divergence time series (1/s) for members 1, 13, 22 and 37.

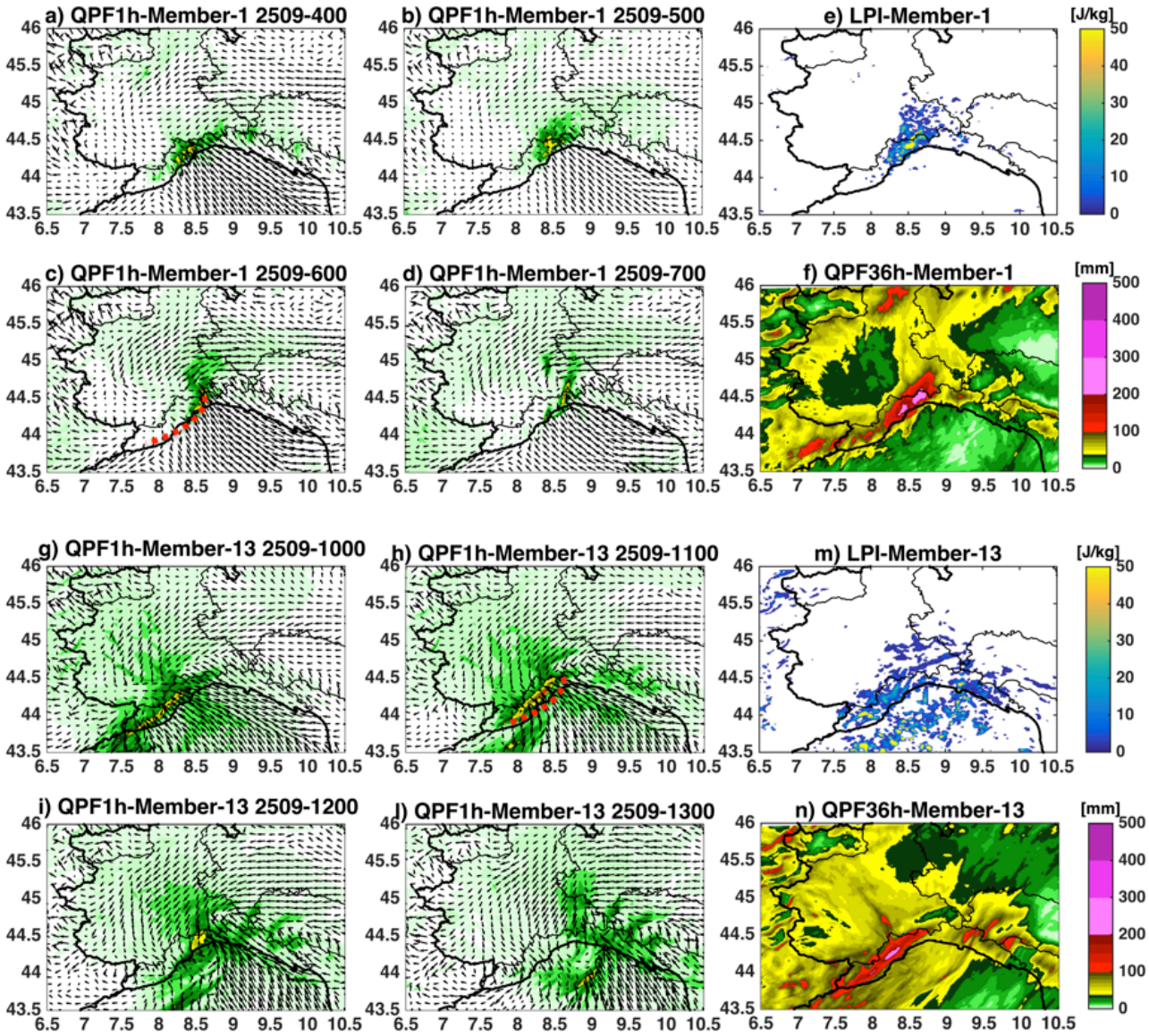

Figure 10: Panels a-d, and g-l show the hourly QPF and 10 m wind fields corresponding to the period with the minimum divergence values in Figure 9 for members 1, and 13 (the convergence line trace in the most active phase is red dashed). Panels e-f, and m-n show the Lightning Potential Index accumulated over the same 4 hours period, and the 36 hour QPF, respectively for members 1, and 13.

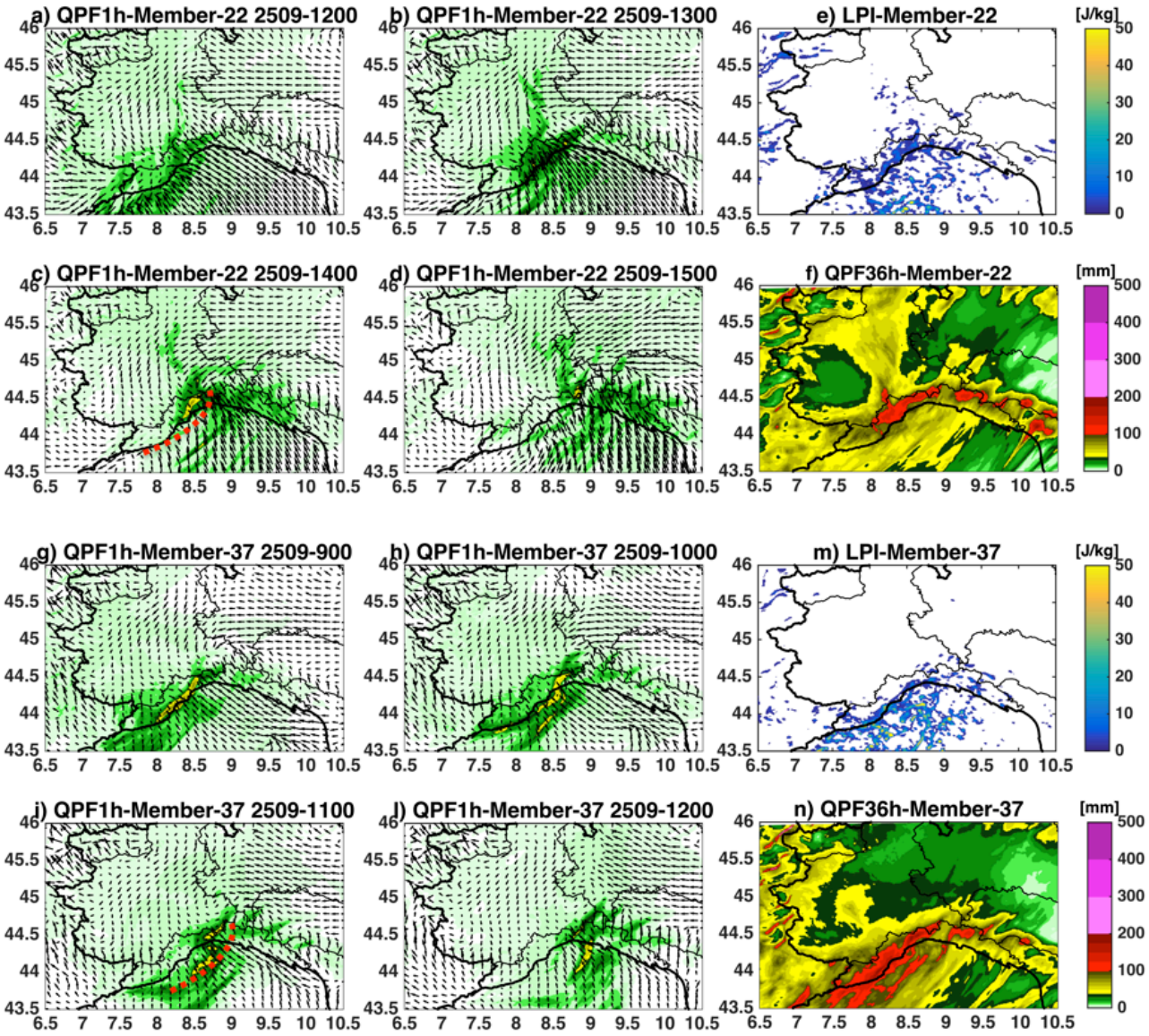

Figure 11: Panels a-d, and g-l show the hourly QPF and 10 m wind fields corresponding to the period with the minimum divergence values in Figure 9 for members 22, and 37 (the convergence line trace in the most active phase is red dashed). Panels e-f, and m-n show the Lightning Potential Index accumulated over the same 4 hours period, and the 36 hour QPF, respectively for members 22, and 37.

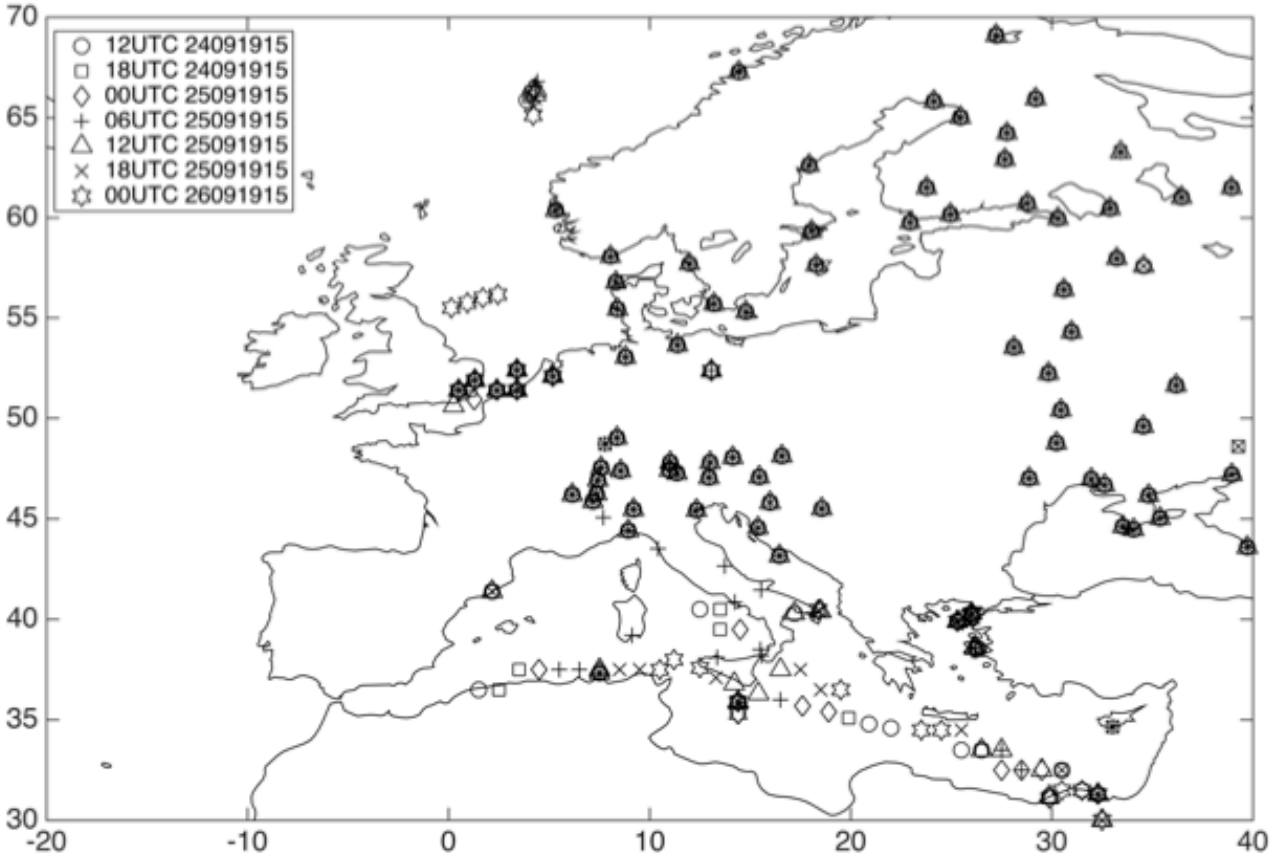

Figure 12: surface pressure stations assimilated every six hours in the period 12UTC 24th September 1915 - 00UTC 26th September 1915.

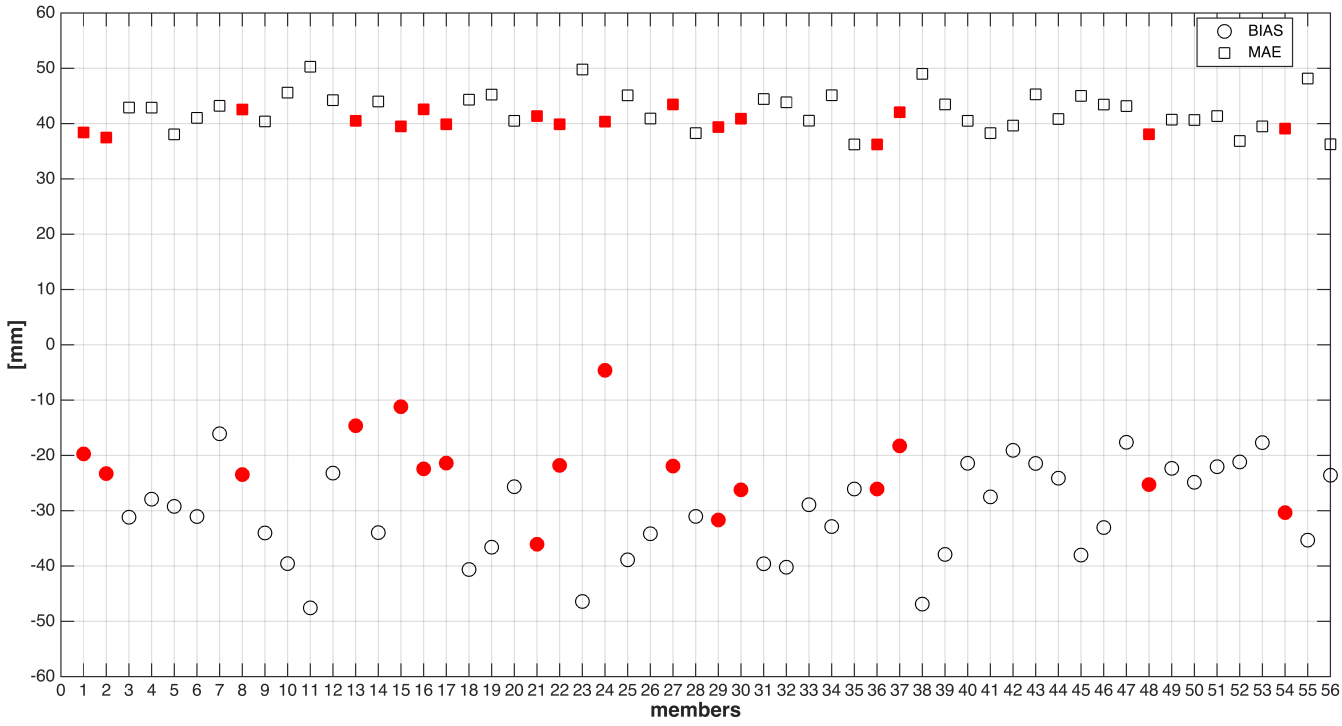

Figure 13: rainfall depth BIAS and MAE for each d03-1km WRF member. Red markers represent the 17 members producing robust and persisting convergence lines over the Liguria Sea.

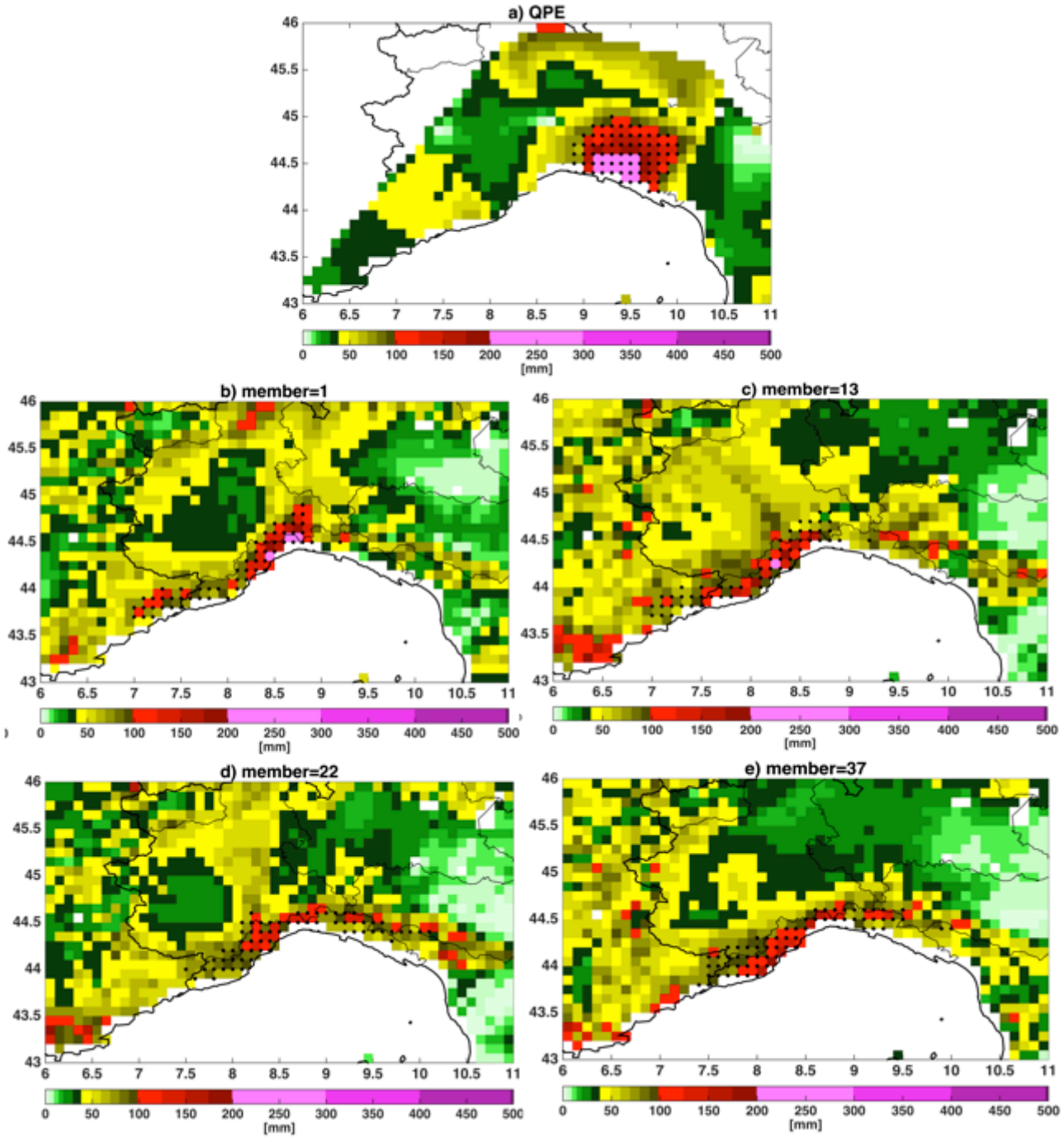

Figure 14: QPE regridded at 10 km grid spacing (panel a) and QPF from members 1 (panel b), 13 (panel c), 22 (panel d) and 37 (panel e), regridded at 10 km grid spacing (lower panels). Dots identify the areas of paired clusters.

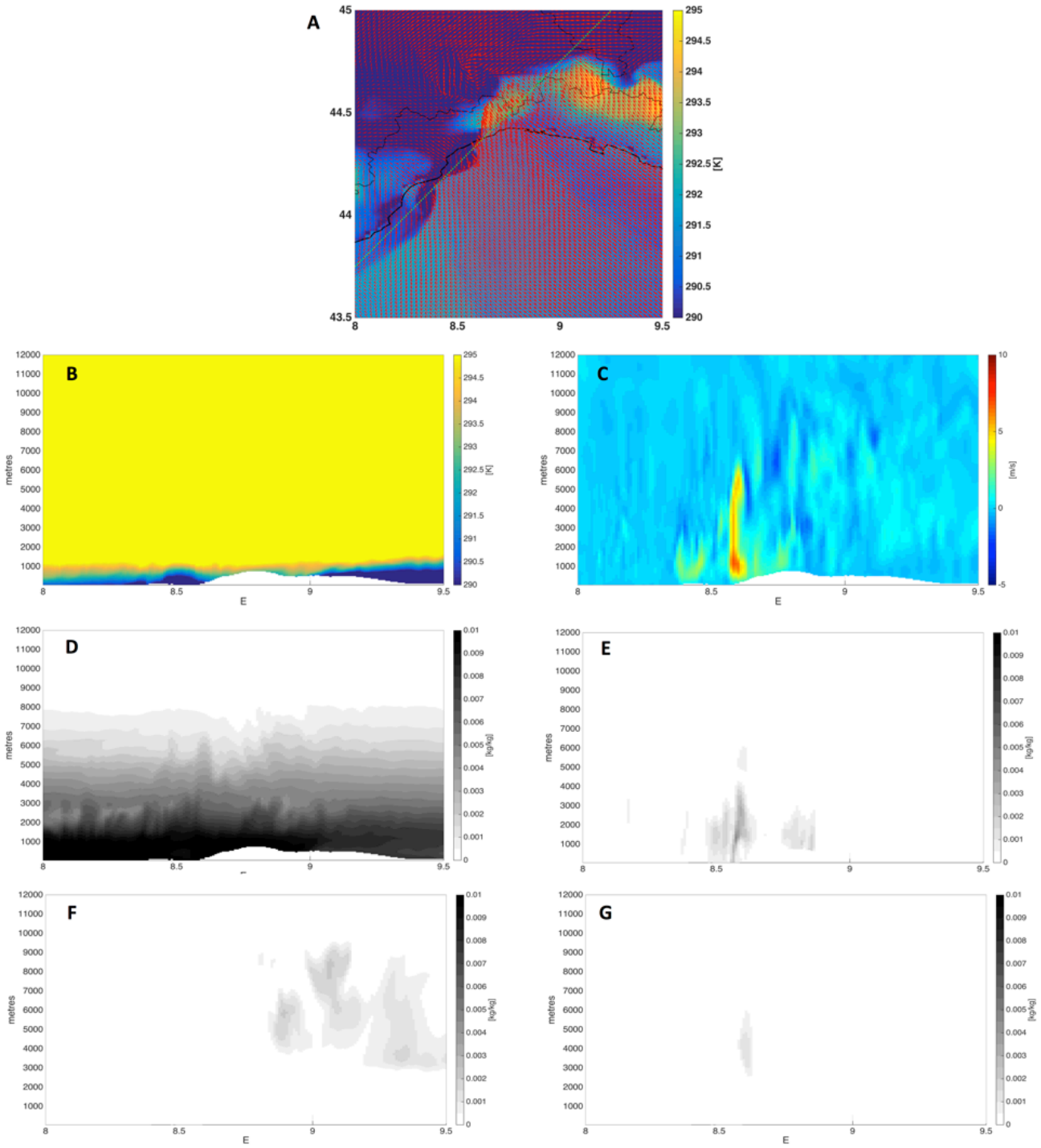

Figure 15: Member 1, 06UTC on 25th September 1915. Panel a shows the 2 m potential temperature field, together with the 10 m horizontal wind vector field. Panels b to g show, instead, potential temperature, vertical velocity, water vapour, rain water, snow, and graupel mixing ratios along the cross section corresponding to the green dotted line shown in panel a.